UNIVERSITÀ
DEGLI STUDI
FIRENZE

DOTTORATO DI RICERCA IN AREA DEL FARMACO
E TRATTAMENTI INNOVATIVI

Ciclo XXVIII

COORDINATORE Prof.ssa Elisabetta Teodori

Hyperpolarization-activated Cyclic Nucleotide gated (HCN) channels as promising new target for neuropathic pain treatment

Settore scientifico disciplinare BIO/14

Dottorando
Dott. Francesco Resta

Tutore
Prof. Guido Mannaioni

Coordinatore
Prof.ssa Elisabetta Teodori

ANNI 2012-2015

anche domani…

Contents

I. Introduction

1. Pain

The International Association for the Study of Pain's define pain as: "an unpleasant sensory and emotional experience associated with actual or potential tissue damage, or described in terms of such damage." (Bonica, 1979)

Pain is a conscious experience that results from brain activity in response to a noxious stimulus and engages the sensory, emotional and cognitive processes of the brain. In general, we can distinguish two dimensions or components of pain, the sensory-discriminative and the affective-emotional

Pricking, burning, aching, stinging describes the unpleasant sensory and soreness are among the most distinctive of all the sensory modalities. As with the other somatic sensory modalities - touch, pressure, and position sense - pain serves an important protective function, alerting us to injuries that require evasion or treatment. In children born with insensitivity to pain, severe injuries often go unnoticed and can lead to permanent tissue damage. Yet pain is unlike other somatic sensory modalities, or vision, hearing, and smell in that it has an urgent and primitive quality, possessing both affective and emotional components. The perception of pain is subjective and is influenced by many factors. An identical sensory stimulus can elicit quite distinct responses in the same individual under different conditions. Many wounded soldiers, for example, do not feel pain until they have been removed from the battlefield; injured athletes are often not aware of pain until a game is over. There are no purely “painful” stimuli, sensory stimuli that invariably elicit the perception of pain in all individuals. Indeed, pain is not the direct expression of a sensory event but rather the product of elaborate processing by the brain of a variety of neural signals (Kandel et al., 2013). The inability to communicate verbally does not negate the possibility that an individual is experiencing pain and is in need of appropriate pain-relieving treatment. Each individual learns the application of the word through experiences related to injury in early life. Accordingly, pain is that experience we associate with actual or potential

tissue damage. It is unquestionably a sensation in a part or parts of the body, but it is also always unpleasant and therefore also an emotional experience. Many people report pain in the absence of tissue damage or any likely pathophysiological cause; usually this happens for psychological reasons. There is usually no way to distinguish their experience from that due to tissue damage if we take the subjective report. If they regard their experience as pain, and if they report it in the same ways as pain caused by tissue damage, it should be accepted as pain (Merskey and Bogduk, 1994).

When pain is experienced it can be acute, persistent, or in extreme cases chronic. Persistent pain characterizes many clinical conditions and is usually the reason that patients seek medical attention. Pain is highly individual and its subjective nature is one of the factors that make it so difficult to define objectively and to treat clinically. Our sensory systems provide the means by which we perceive the external world, remain alert, form a body image, and regulate our movements. Sensations arise when external stimuli interact with some of the billion sensory receptors that innervate every organ of the body. The information detected by these receptors is conveyed to the brain as trains of action potentials traveling along individual sensory axons. These messages are analyzed centrally by several million sensory neurons performing different, specific functions in parallel. Each sensory neuron extracts highly specific and localized information about the external or internal environment and in turn has a specific effect on sensation and cognition because it projects to specific places in the brain that have specific sensory functions. All sensory systems respond to four elementary features of stimuli modality, location, intensity, and duration. The diverse sensations we experience the sensory modalities reflect different forms of energy that are transformed by receptors into depolarizing or hyperpolarizing electrical signals called receptor potentials. Receptors specialized for particular forms of energy, and sensitive to particular ranges of the energy bandwidth, allow humans to sense many kinds of mechanical, thermal, chemical, and electromagnetic events. To maintain the specificity of each modality within the nervous system, receptor axons are segregated into discrete anatomical pathways that terminate in unimodal nuclei. After about a dozen synaptic steps in each sensory system, neural activity converges on neuronal groups whose function is polymodal and more directly cognitive. The location and spatial dimensions of a stimulus are conveyed through each receptor's receptive field,

the precise area in the sensory domain in which stimulation activates the receptor. The intensity and duration of stimulation are represented by the amplitude and time course of the receptor potential and by the total number of receptors activated. In the brain, intensity is encoded in the frequency of firing, which is proportional to the strength of the stimulus. The temporal features of a stimulus, such as duration and changes in magnitude, are signaled by the dynamics of the spike train. The pattern of action potentials in peripheral nerves and in the brain gives rise to sensations whose qualities can be measured directly using a variety of psychophysical paradigms such as magnitude estimation and signal detection and discrimination tasks. Reaction times to stimuli also provide a means for measuring the intensity of stimulation and the ease of sensory discrimination in both human and animal subjects. The neural activity in a set of thousands or millions of neurons should be thought of as coordinated activity that conveys a "neural image" of specific properties of the external world. Sensory information in the central nervous system is processed in stages, in the sequential relay nuclei of the spinal cord, brain stem, thalamus, and cerebral cortex (Kandel et al., 2013). The sensation of pain is a normal response to injury or disease and is a result of normal physiological processes within the nociceptive system, with its complex of stages previously described. There may also be other manifestations of pain related to tissue injury including hyperalgesia, an exaggerated response to a noxious stimulus, and allodynia, the perception of pain from normally innocuous stimuli. Hyperalgesia and allodynia are the result of changes in either the peripheral or central nervous systems, referred to as peripheral or central sensitization, respectively. Genetic and environmental factors contribute to sensitization resulting in persistent (chronic) pain in some individuals even after healing has taken place. Nociceptors not only signal acute pain, but when chronically sensitized contribute to persistent pathological pain disorders from previous injury or ongoing disease. Chronic pain is also characterized by the abnormal state and function of the spinal cord neurons, which become hyperactive. This hyperactivity is the result of increased transmitter release by spontaneously active primary afferent neurons and an increased responsiveness of postsynaptic receptors. A hyper-excitable state of synaptic transmission at the dorsal horn is further maintained by release of biologically active factors from activated glia. The state of hyperexcitability is aggravated by the loss of inhibitory interneurons

involved in the modulation of pain. Under normal circumstances the nociceptive sensory system returns to a normal functional state as soon as healing takes place (Kandel et al., 2013). However, many features of sensitization persist and are manifest as chronic pain and hyperalgesia, especially when the nervous system itself is injured leading to chronic neuropathic pain. Imaging studies have shown that chronic pain is accompanied by permanent structural alterations in specific brain areas that play a crucial role in nociception. Clinical practice should aim to decrease the intensity of acute pain in an effort to reduce or prevent permanent changes in the nervous system that may result in chronic pain. Multimodal therapy, which involves drug and non-drug treatments and rational combinations of drugs that work by different mechanisms, are important in providing optimal relief of pain and reducing the probability of persistent changes that characterize chronic pain. Nociception is the process by which information about a noxious stimulus is conveyed to the brain. The total sum of neural activity that occurs prior to the cognitive processes, allow humans to identify a sensation as pain. Nociception is necessary but not sufficient for the experience of pain. The goal of pain therapies is to relieve pain whenever possible: from nociception to the conscious experience as well as to decrease the emotional response to the unpleasant experience (Gureje, 2007).

1.1 Classification of pain

In 1994, responding to the need for a more useful system for describing pain, the International Association for the Study of Pain (IASP) classified pain according to specific characteristics: (1) region of the body involved (e.g. abdomen, lower limbs), (2) system whose dysfunction may be causing the pain (e.g., nervous, gastrointestinal), (3) duration and pattern of occurrence, (4) intensity and time since onset, and (5) etiology (Main and Spanswick, 2000). However, this system has been criticized by Clifford J. Woolf and others as inadequate for guiding research and treatment. Woolf suggests three classes of pain: (1) nociceptive pain, (2) inflammatory pain which is associated with tissue damage and the infiltration of immune cells, and (3) pathological pain which is a disease state caused by damage to the nervous system or by its

abnormal function (e.g. fibromyalgia, irritable bowel syndrome, tension type headache, etc.) (Woolf, 2010).

Classifying pain is helpful to guide assessment and treatment. There are many ways to classify pain and classifications may overlap. The common types of pain include nociceptive, inflammatory and neuropathic pain. Nociceptive pain: represents the normal response to noxious insult or injury of tissues such as skin, muscles, visceral organs, joints, tendons, or bones. This type of pain include both somatic pain, such as musculoskeletal and cutaneous pain that are often well localized, and visceral pain, that comprise hollow organs and smooth muscle. Inflammatory pain is the result of activation and sensitization of the nociceptive pain pathway by a variety of mediators released at a site of tissue inflammation. The mediators that have been implicated as key players are pro-inflammatory cytokines, chemokines, reactive oxygen species, vasoactive amines, lipids, ATP, acid, and other factors released by infiltrating leukocytes, vascular endothelial cells, or tissue resident mast cells. Examples of inflammatory pain include appendicitis, rheumatoid arthritis, inflammatory bowel disease, and herpes zoster. Finally, neuropathic pain is initiated or caused by a primary lesion or disease in the somatosensory nervous system. Sensory abnormalities range from deficits perceived as numbness to hypersensitivity (hyperalgesia or allodynia), and to paresthesia such as tingling. Examples of neuropathic pain are diabetic neuropathy, post herpetic neuralgia, spinal cord injury pain, phantom limb (post-amputation) pain, and post-stroke central pain. (Kennedy, 2007)

Another way to classify pain is by clinical implications. Pathological processes never occur in isolation and consequently more than one mechanism may be present and more than one type of pain may be detected in a single patient; for example, it is known that inflammatory mechanisms are involved in neuropathic pain. There are well-recognized pain disorders that are not easily classifiable. Our understanding of their underlying mechanisms is still rudimentary though specific therapies for those disorders are well known; they include cancer pain, migraine and other primary headaches and widespread pain of the fibromyalgia type. Pain Intensity can be broadly categorized as mild, moderate and severe. It is common to use a numeric scale to rate

pain intensity where 0 = no pain and 10 is the worst pain imaginable (Mild: <4/10, Moderate: 5/10 to 6/10, Severe: >7/10). (de C Williams et al., 2000).

Pain is usually transitory, lasting only until the noxious stimulus is removed or the underlying damage or pathology has healed, but some painful conditions, such as rheumatoid arthritis, peripheral neuropathy, cancer and idiopathic pain, may persist for years. Pain that lasts a long time is called chronic, and pain that resolves quickly is called acute. Traditionally, the distinction between acute and chronic pain has relied upon an arbitrary interval of time from onset. The two most commonly used markers being 3 months and 6 months since the onset of pain (Turk and Okifuji, 2001), though some theorists and researchers have placed the transition from acute to chronic pain at 12 months. Others apply acute to pain that lasts less than 30 days, chronic to pain of more than six months' duration, and sub acute to pain that lasts from one to six months (Main and Spanswick, 2000). A popular alternative definition of chronic pain, involving no arbitrarily fixed durations, is "pain that extends beyond the expected period of healing" (Weiner, 2002).

1.2 Pain pathways

Nociceptive information is transmitted from the spinal cord to the thalamus. Five major ascending pathways convey nociceptive information: the spinothalamic, spinoreticular, spinomesencephalic, cervicothalamic, and spinohypothalamic tracts contribute to the central processing of nociceptive information. The spinothalamic tract is the most prominent ascending nociceptive pathway in the spinal cord. It includes the axons of nociception-specific, thermosensitive, and wide-dynamic-range neurons in laminae I and V of the dorsal horn. These axons cross the midline of the spinal cord at their segment of origin and ascend in the anterolateral white matter before terminating in thalamic nuclei (Kandel et al., 2013)(Figure 1).

The spinothalamic tract has a crucial role in the transmission of nociceptive information. Electrical stimulation of the tract is sufficient to elicit the sensation of

pain; conversely, lesioning this tract (anterolateral cordotomy) can result in a marked reduction in pain sensation on the side of the body contralateral to that of the lesion.

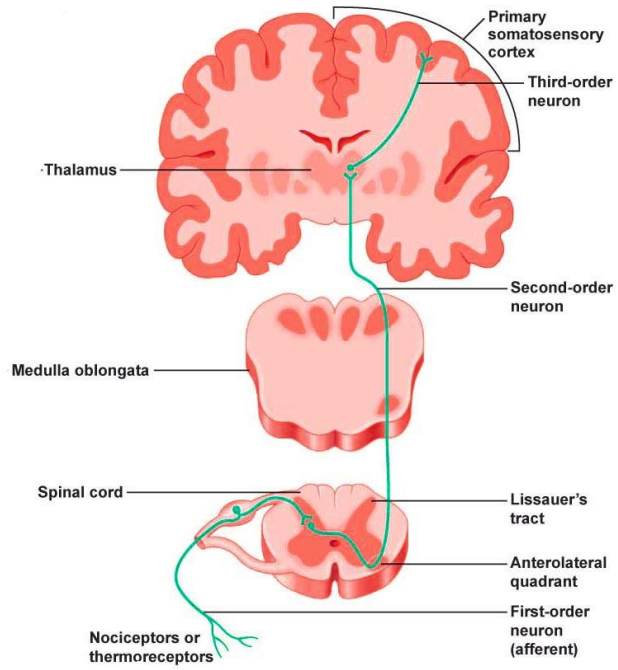

Figure 1 The Spinothalamic tract from Pearsn Education 2011.

The spinoreticular tract contains the axons of projection neurons in laminae VII and VIII. This tract ascends in the anterolateral quadrant of the spinal cord and terminates in both the reticular formation and the thalamus. The axons of spinoreticular tract neurons do not cross the midline. The spinomesencephalic (or spinoparabrachial) tract contains the axons of projection neurons in laminae I and V. Information transmitted along this tract is thought to contribute to the affective component of pain. This tract projects in the anterolateral quadrant of the spinal cord to the mesencephalic reticular formation and periaqueductal gray matter, axons in this tract also project to the parabrachial nucleus. Neurons of the parabrachial nucleus project to the amygdala, a key nucleus of the limbic system that regulates emotional states. Many of the axons of this pathway course through the dorsal part of the lateral funiculus rather than in the anterolateral quadrant. In surgical procedures designed to relieve pain, such as anterolateral cordotomy, the sparing of these fibers may explain the persistence or recurrence of pain after surgery. The cervicothalamic tract runs in the lateral white

matter of the upper two cervical segments of the spinal cord and contains the axons of neurons of the lateral cervical nucleus, which receives input from neurons in laminae III and IV of the dorsal horn. Most axons in the cervicothalamic tract cross the midline and ascend in the medial lemniscus of the brain stem, terminating in midbrain nuclei and in the ventroposterior lateral and posteromedial nuclei of the thalamus. The spinohypothalamic tract contains the axons of neurons found in laminae I, V, and VIII of the dorsal horn in the spinal cord. These axons project to hypothalamic nuclei that serve as autonomic control centers involved in the regulation of the neuroendocrine and cardiovascular responses that accompany pain syndromes. Laminae III and IV send their axons directly into the several thalamic nuclei that participate in the central processing of nociceptive information. Two of the most important regions of the thalamus are the lateral and medial nuclear groups. The lateral nuclear group comprises the ventroposterior medial nucleus, the ventroposterior lateral nucleus and the posterior nucleus. These three nuclei receive inputs through the spinothalamic tract from nociception-specific and wide-dynamic-range neurons in laminae I and V of the dorsal horn. The lateral thalamus is thought to be concerned with the processing of information about the precise location of an injury, information usually conveyed to consciousness as acute pain. Consistent with this view, neurons in the lateral thalamic nuclei have small receptive fields, matching those of the presynaptic spinal neurons. Injury to the spinothalamic tract and its thalamic targets causes a severe form of pain termed central pain. An infarct in a small region of the ventroposterolateral thalamus produces the perception of a spontaneous burning pain, together with other abnormal sensations (called dysesthesias) that are perceived as originating from diverse regions of the body. This constellation of abnormal percepts has been termed the Dejerine Roussy syndrome. Electrical stimulation of the thalamus can also result in intense pain. In one dramatic clinical case, electrical stimulation of the thalamus rekindled sensations of angina pectoris that were so realistic that the anesthesiologist thought the patient was experiencing a heart attack. This and other clinical observations suggest that in chronic pain conditions there is a fundamental change in thalamic and cortical circuitry. The medial nuclear group of the thalamus comprises the central lateral nucleus of the thalamus and the intralaminar complex. Its major input is from neurons in laminae VII and VIII of the dorsal horn. The pathway to the medial thalamus was

the first spinothalamic projection evident in the evolution of mammals and is therefore known as the paleospinothalamic tract. It is also sometimes referred to as the spinoreticulothalamic tract because it includes indirect connections through the reticular formation of the brain stem. The projection from the lateral thalamus to the ventroposterior lateral and medial nuclei is most developed in primates, and is termed the neospinothalamic tract. Many neurons in the medial thalamus respond optimally to noxious stimuli and project widely to the basal ganglia and different cortical areas (Kandel et al., 2013).

Somatosensory information flows from the spinal cord to the thalamus through parallel pathways. The nerve fibers that convey the various somatosensory submodalities from each dermatome are bundled together in the peripheral nerves as they enter the dorsal root ganglia. However, as the fibers exit the ganglia and approach the spinal cord, the large- and small-diameter fibers separate into medial and lateral divisions. The medial division includes large, myelinated Aα and Aβ fibers that transmit proprioceptive and cutaneous information from a dermatome. The lateral division includes small thinly myelinated Aδ and unmyelinated C fibers that transmit noxious, thermal, and visceral information from the same dermatome. After entering the spinal cord, the afferent fibers become further segregated according to modality and terminate on different functional sets of neurons in the gray matter of the same or adjacent spinal segments. In addition, the Aα and Aβ fibers send a major branch to the medulla through the dorsal columns. The gray matter in each spinal segment is divided into three functionally distinct regions: the dorsal and ventral horns and an intermediate zone. As a general rule the largest fibers (Aα) terminate in or near the ventral horn, the medium-size fibers (Aβ) from the skin and muscle terminate in intermediate layers of the dorsal horn, and the smallest fibers (Aδ and C) terminate in the most dorsal portion of the spinal gray matter. The spinal gray matter is further subdivided into 10 laminae (or layers), numbered I to X from dorsal to ventral, based on differences in cell and fiber composition. Lamina I consists of a thin layer of neurons capping the dorsal horn of the spinal cord and pars caudalis of the spinal trigeminal nucleus. Individual neurons of lamina I receive monosynaptic inputs from small myelinated fibers (Aδ) or unmyelinated C fibers of a single type and therefore transmit information about noxious, thermal, or visceral stimuli. Inputs from warm,

cold, itch, and pain receptors have been identified in lamina I, and some neurons have unique cellular morphologies. Lamina I neurons generally have small receptive fields localized to one dermatome. Neurons in laminae II and III are interneurons that receive inputs from Aδ and C fibers, and make excitatory or inhibitory connections to neurons in lamina I, IV, and V that project to higher brain centers. The dendrites of neurons in laminae III to V are the main targets of the large myelinated sensory (Aβ) fibers from cutaneous mechanoreceptors. Neurons in lamina V typically respond to more than one modality, low-threshold mechanical stimuli, visceral stimuli or noxious stimuli and have therefore been named wide-dynamic-range neurons. Visceral C fibers have widespread projections in the spinal cord that terminate ipsilaterally in laminae I, II, V, and X; some also cross the midline and terminate in lamina V and X of the contralateral gray matter. The extensive spinal distribution of visceral C fibers appears to be responsible for the poor localization of visceral pain sensations. Afferents from the pelvic viscera make important connections to cells in the central gray matter (lamina X) of spinal segments L5 and S1. Lamina X neurons in turn project their axons along the midline of the dorsal columns to the nucleus gracilis in a postsynaptic dorsal column pathway for visceral pain. Primary afferent fibers that terminate in the deepest laminae in the ventral horn feed back information from proprioceptors that is required for somatic motor control, such as spinal reflexes. (Kandel et al., 2013).

As there are ascending pathways to the brain that initiates the conscious realization of pain, there are also descending pathway, which modulates pain sensation. The brain can request the release of specific hormones or chemicals that can have analgesic effects, which can reduce or inhibit pain sensation. The areas of the brain that stimulates the release of these mediators are the periaqueductal gray (PAG) and the nucleus raphe magnus (NRM) (Mayer et al., 1971). Stimulation of the periaqueductal gray matter of the midbrain activates enkephalin-releasing neurons that project to the raphe nuclei in the brainstem. 5-HT (serotonin) released from the raphe nuclei descends to the dorsal horn of the spinal cord where it forms excitatory connections with the "inhibitory interneurons" located in Laminae II (aka the substantia gelatinosa). When activated, these interneurons release either enkephalin or dynorphin (endogenous opioid neurotransmitters), which bind to mu opioid receptors on the axons of incoming C and Aδ fibers carrying pain signals from nociceptors activated in

the periphery. The activation of the mu-opioid receptor inhibits the release of substance P from these incoming first-order neurons and, in turn, inhibits the activation of the second-order neuron that is responsible for transmitting the pain signal up the spinothalamic tract to the ventroposteriolateral nucleus (VPL) of the thalamus. The nociceptive signal was inhibited before it was able to reach the cortical areas that interpret the signal as "pain" (such as the anterior cingulate). This is sometimes referred to as the Gate control theory of pain and is supported by the fact that electrical stimulation of the PAG results in immediate and profound analgesia (Basbaum and Fields, 1978).

1.2.1 Dorsal root ganglia

The primary sensory neurons of the somatosensory system are clustered in the dorsal root ganglia (DRG) (Figure 2). Somatosensory information from the skin, muscles, joint capsules, and viscera is conveyed by dorsal root ganglion neurons innervating the limbs and trunk or by trigeminal sensory neurons that innervate cranial

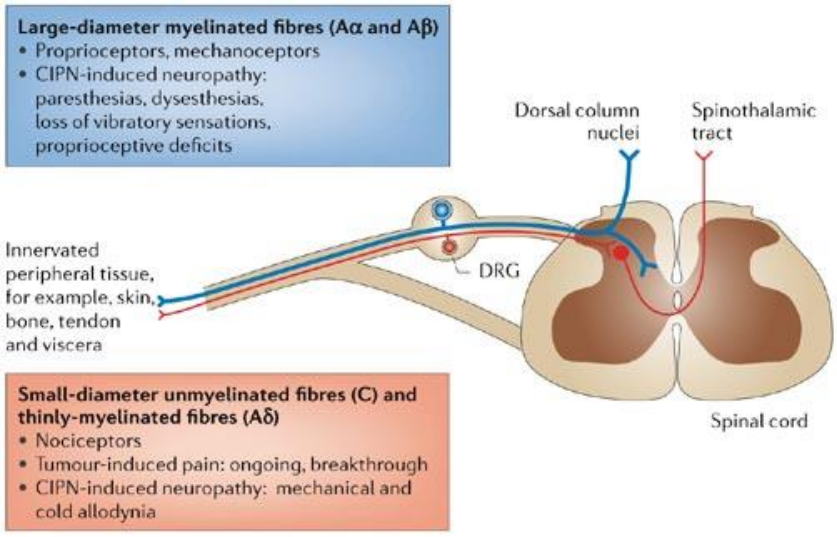

Figure 2 Dorsal root ganglion from Nature Reviews Neuroscience 2006

structures (the face, lips, oral cavity, conjunctiva, and dura mater). The cell body of a DRG neuron lies in a ganglion on the dorsal root of a spinal or cranial nerve. These sensory neurons perform two major functions: the transduction and encoding of stimuli into electrical signals and the transmission of those signals to the central nervous

system. DRG neurons originate from the neural crest and are intimately associated with the nearby segment of the spinal cord. DRG neurons are a type of bipolar cell, called pseudo-unipolar cells. The axon of a dorsal root ganglion neuron has two branches, one projecting to the periphery and one projecting to the central nervous system. The peripheral terminals of different neurons contain receptors specialized for particular kinds of stimuli. They differ in receptor morphology and stimulus selectivity. The central branches terminate in the spinal cord or brain stem, forming the first synapses in somatosensory pathways. Thus, the axon of each DRG cell serves as a single transmission line with one polarity between the receptor terminal and the central nervous system. This axon is called the primary afferent fiber. Individual primary afferent fibers innervating a particular region of the body, such as the thumb or fingers, are grouped together into bundles or fascicles of axons forming the peripheral nerves. They are guided during development to a specific location in the body by various trophic factors. The peripheral nerves also include motor axons innervating nearby muscles, blood vessels, glands, or viscera. Damage to peripheral nerves or their targets in the brain may produce sensory deficits in more than one somatosensory submodality (Kandel et al., 2013).

1.2.2 Nociceptors

Nociceptors are the neurons that transduct the various pain stimuli in electrical signals. They respond directly to mechanical and thermal stimuli, and indirectly to other stimuli by means of chemicals released from cells in the traumatized tissue. Nociceptors signal impending tissue injury and, more importantly, they provide a constant reminder of tissues that are already injured and must be protected. Nociceptors in the skin, muscle, joints, and visceral receptors fall into two broad classes based on the myelination of their afferent fibers. Nociceptors innervated by Aδ fibers produce short-latency pain that is described as sharp and pricking. The majority are called mechanical nociceptors because they are excited by sharp objects that penetrate, squeeze, or pinch the skin. Many of these Aδ fibers also respond to noxious heat that can burn the skin. Nociceptors innervated by C fibers produce dull, burning pain that is diffusely localized and poorly tolerated. The most common type are

polymodal nociceptors that respond to a variety of noxious mechanical, thermal, and chemical stimuli, such as pinch or puncture, noxious heat and cold, and irritant chemicals applied to the skin. Electrical stimulation of these fibers in humans evokes prolonged sensations of burning pain. In the viscera nociceptors are activated by distension or swelling, producing sensations of intense pain. Many organs, including skin and subcutaneous structures such as joints and muscles, possess specialized sensory receptors that are activated by noxious insults. Unlike the specialized somatosensory receptors for light touch and pressure, most of these nociceptors are simply the free nerve endings of primary sensory neurons. There are three main classes of nociceptors: thermal, mechanical, and polymodal and a more enigmatic fourth class, termed silent nociceptors. Thermal nociceptors are activated by extremes in temperature, typically greater than 45 °C or less than 5 °C. They are the peripheral endings of small diameter, thinly myelinated Aδ axons that conduct action potentials at speeds of 5 to 30 m/s. Mechanical nociceptors are activated optimally by intense pressure applied to the skin; they too are the endings of thinly myelinated Aδ axons. Polymodal nociceptors can be activated by high-intensity mechanical, chemical, or thermal (both hot and cold) stimuli. This class of nociceptors is found at the ends of small-diameter, unmyelinated C axons that conduct more slowly, at speeds less than 1.0 m/s. These three classes of nociceptors are widely distributed in skin and deep tissues and are often coactivated. When a hammer hits your thumb, you initially feel a sharp pain (“first pain”) followed by a more prolonged aching and sometimes burning pain (“second pain”). The fast sharp pain is transmitted by Aδ fibers that carry information from damaged thermal and mechanical nociceptors. The slow dull pain is transmitted by C fibers that convey signals from polymodal nociceptors. Silent nociceptors are found in the viscera. This class of receptors is not normally activated by noxious stimulation; instead, inflammation and various chemical agents dramatically reduce their firing threshold. Their activation is thought to contribute to the emergence of secondary hyperalgesia and central sensitization, two prominent pain syndromes. Noxious stimuli depolarize the bare nerve endings of afferent axons and generate action potentials that are propagated centrally. The membrane of the nociceptor contains receptors that convert the thermal, mechanical, or chemical energy of noxious stimuli into a depolarizing electrical potential. One protein is a member of

a large family of so-called transient receptor potential (TRP) ion channels. TRPV1 is expressed selectively by nociceptive neurons and mediates the pain-producing actions of capsaicin, the active ingredient of hot peppers, and many other pungent chemicals. The TRPV1 channel is also activated by noxious thermal stimuli, which suggests that it normally transduces the sensation of painful heat. In addition, TRPV1-mediated membrane currents are enhanced by a reduction in pH, a characteristic of the chemical milieu of inflammation. Additional members of the TRP channel family are expressed by nociceptive neurons, and the variety of TRP channels in nociceptors is thought to underlie the perception of a wide range of temperatures from extreme cold to intense heat. The TRPV2 channel is expressed predominantly in Aδ fiber terminals and is activated by very high temperatures, whereas the TRPM8 channel is activated by low temperatures and by chemicals such as menthol. In addition to this constellation of TRP channels, other receptors and ion channels that participate in the transduction of peripheral stimuli are expressed in nociceptive sensory endings. Nociceptors selectively express tetrodotoxin-resistant Na+ channels. One Na+ channel (SCN9A, also called NaV1.7) plays a key role in the perception of pain in humans, as revealed by the rare pain-insensitive individuals who possess mutations in the corresponding gene. One class of mutations inactivates the SCN9A channel and results in a complete inability to sense pain. However, in all other respects these individuals are healthy and exhibit normal sensory responses to touch, mild temperature, proprioception, tickle, and pressure. A second class of mutations in the SCN9A gene changes the inactivation kinetics of this channel; individuals with these mutations exhibit an inherited condition called paroxysmal extreme pain disorder, characterized by rectal, ocular, and submandibular pain. Nociceptors also express an ionotropic purinergic receptor, PTX3, that is activated by adenosine triphosphate (ATP) released from peripheral cells after tissue damage (Kandel et al., 2013). Another important family of channels expressed by nociceptors is the Hyperpolarization-activated Cyclic Nucleotide gated (HCN) channels, that are cation channels responsible for resting membrane potential (RMP), pacemaker activity and neuronal excitability. Finally, nociceptors expressed a

huge variety of receptors and channels, providing attractive targets for the development of drugs with actions selective for nociceptive sensory neurons.

The uncontrolled activation of nociceptors is associated with several pathological conditions. Allodynia and hyperalgesia are two common pain states that reflect changes in nociceptor activity. Patients with allodynia feel pain in response to stimuli that are normally innocuous: by a light stroking of sunburned skin, by the movement of joints in patients with rheumatoid arthritis, and even by the act of getting out of bed in the morning after a vigorous workout. Nevertheless, patients with allodynia do not feel pain constantly; in the absence of a peripheral stimulus there is no pain. In contrast, patients with hyperalgesia, an exaggerated response to noxious stimuli, typically report persistent pain in the absence of sensory stimulation. As mentioned before persistent pain can be subdivided into two broad classes, nociceptive and neuropathic. Nociceptive pain results from the activation of nociceptors in the skin or soft tissue in response to tissue injury, and it usually arises from an accompanying inflammation. Sprains and strains produce mild forms of nociceptive pain, whereas arthritis or a tumor that invades soft tissue produces a much more severe nociceptive pain. Neuropathic pain results from direct injury to nerves, in the peripheral or central nervous system and is often accompanied by a burning or electric sensation. Neuropathic pains include the syndromes of reflex sympathetic dystrophy, also called complex regional pain syndrome, and post-herpetic neuralgia, the severe pain experienced by patients after a bout of shingles. Finally neuropathic pains include also phantom limb pain, the pain that occurs after limb amputation (Kandel et al., 2013).

1.3 Neuropathic pain

Neuropathic pain may result from disorders of the peripheral or central nervous system and affect Up to 7% to 8% of the European population, in 5% it may be severe (Torrance et al., 2006). The phrase “neuropathic pain” came into common use only in the last decade and increasingly has been appreciated as a frequent source of chronic pain, the following case represents a classical presentation of a patient with neuropathic pain:

A 47-year-old woman presented for consultation for complaints of pain on the right chest wall. The patient underwent a mastectomy on the right side as a treatment for

cancer 5 years previously. As the surgical pain faded, the patient noted increasing chest-wall pain that extended well beyond the surgical borders. Clothing lightly touching the skin increased the pain. Reconstructive surgery was deferred because of concerns about the ongoing pain. In addition to the ongoing burning pain, the patient also complained of sudden "pain attacks" one to several times a day. These attacks lasted seconds to minutes and were described as debilitating. Examination revealed a well-healed surgical scar. Light stroking of the skin provoked significant pain in an area from the clavicle down to the T8 dermatome. Despite the pain to light tactile stimuli, the patient also had areas of decreased sensibility as demonstrated by the inability to detect a fine probe applied to the skin(Campbell and Meyer, 2006).

The notable features that point to neuropathic processes are widespread pain not otherwise explainable, evidence of sensory deficit, burning pain, pain to light stroking of the skin and attacks of pain without seeming provocation. The liability for pain appears to vary from person to person, from nerve to nerve, between males and females, and even with age. What appears to be the same lesion may induce no pain in one person but severe pain in another. In addition to ongoing pain (i.e., stimulus-independent pain), patients may have heightened pain to stimuli applied to their skin. By definition, neuropathic pain originates from a lesion of the nervous system and innumerable diseases may be the culprits. Examples include autoimmune disease (e.g., multiple sclerosis), metabolic diseases (e.g., diabetic neuropathy), infection (e.g., shingles and the sequel, postherpetic neuralgia), vascular disease (stroke), trauma, and cancer. A rule without apparent exception is that the lesion leading to pain must directly involve the nociceptive pathways (Boivie et al., 1989), indeed lesions of the medial lemniscal system (e.g., dorsal columns) do not induce pain (COOK and BROWDER, 1965). Namely, not all lesions of nociceptive pathways induce pain. A lesion of the peripheral nerve may induce pain, but simply severing dorsal roots seems to have little chance of creating lasting pain (Li et al., 2000). Lesions of the brainstem and thalamus carry a risk of causing pain if the nociceptive pathways are involved (Wall et al., 2006). In nearly all of these cases, there is the paradoxical juxtaposition of ongoing pain and a sensory deficit to noxious stimulation (even when hyperalgesia is present). Lesions confined to the cortex appear not to be associated with abnormal

pain (but it is also unclear whether lesions confined to the cerebral cortex induce deficits of pain sensibility

A rich variety of diseases of the nervous system are associated with pain (Wall et al., 2006). The offending lesion may involve a simple axotomy (cutting of the nerve) or merely nerve entrapment. Ongoing pain may be the only manifestation, but in many cases, hyperalgesia with pain to light-stroking stimuli (allodynia) may be manifest. In some cases, there is striking cooling hyperalgesia, where mild lowering of skin temperature exacerbates the pain (Campbell and Meyer, 2006).

One of the classic examples of neuropathic pain is Tic douloureux. Without treatment, this is a debilitating disorder that involves attacks of severe pain in the facial area (also referred to as trigeminal neuralgia). Often there is little or no pain between attacks. Light touching of the skin in a so-called trigger zone suffices to evoke an attack. The disease appears to be associated with mechanical distortion at the entry zone of the nerve root to the brainstem. Demyelination may be seen at the compression site. Nerve compression from an aberrant blood vessel is one of the more common causes (Elias and Burchiel, 2002). Another classical neuropathic pain condition is painful diabetic neuropathy (Dyck et al., 2000). Diabetes often causes a length-dependent neuropathy (meaning that the longest axons in the peripheral nerve are most vulnerable). Patients report bilateral burning pain in the toes and feet. Quantitative sensory testing reveals decreased pain sensibility (with or without decreased touch sensibility) (Campbell and Meyer, 2006).

In addition, infections could lead to neuropathic pain. An example is the postherpetic neuralgia, a complication of shingles resulting from an activation of the herpes zoster virus that takes up residence in the DRG after a chickenpox infection. The shingles eruption consists of blisters that follow the dermatome(s) of one or more spinal nerves. The blisters heal in time, but the pain may continue. Allodynia is a particularly prominent feature of postherpetic neuralgia. Allodynia may be present even with loss of C-fiber innervation of the epidermis.

1.3.1 Drugs and treatments for neuropathic pain

The clinical manifestations of neuropathic pain vary with the type of disease, these variations suggest different mechanisms. Differences in mechanism may also be

reflected in responses to therapy. Tic douloureux responds nicely to treatment with the anticonvulsant carbamazepine. Responses to carbamazepine for other conditions are typically disappointing. Painful diabetic neuropathy leads to ongoing pain, but allodynia is distinctly unusual, and cooling may relieve pain. In contrast, allodynia is prominent in traumatic neuropathy and cooling often causes severe pain (Campbell and Meyer, 2006). Neuropathic pain can be very difficult to treat with only some 40-60% of people achieving partial relief (Bennett and Xie, 1988; Dworkin et al., 2010). Favored treatments are certain antidepressants (tricyclic antidepressant and serotonin-norepinephrine reuptake inhibitors), anticonvulsants (pregabalin and gabapentin), and topical lidocaine. Opioid analgesics are recognized as useful agents but are not recommended as first line treatments (Dworkin et al., 2010). Pregabalin and gabapentin are first-line medications for diabetic neuropathy. The anticonvulsants carbamazepine and oxcarbazepine are effective in trigeminal neuralgia instead lamotrigine does not appear to be effective for neuropathic pain (Wiffen et al., 2013). Dual serotonin-norepinephrine reuptake inhibitors such as duloxetine, venlafaxine, and milnacipran, as well as tricyclic antidepressants such as amitriptyline, nortriptyline, and desipramine are considered first-line medications (Dworkin et al., 2010). While amitriptyline and desipramine has been used as a first line treatment, the quality of evidence to support their use is poor (Hearn et al., 2014; Moore et al., 2012). Bupropion has been found to have efficacy in the treatment of neuropathic pain (Semenchuk and Davis, 2000; Semenchuk et al., 2001; Shah and Moradimehr, 2010).

A different approach is the neuromodulation through implanted devices. Unfortunately, these innovative treatments are expensive and carry the risk of complications. Available studies have focused on conditions having a different prevalence than neuropathic pain patients in general. More research is needed to define the range of conditions that they might benefit. One of the better characterized treatment is the deep brain stimulation, consisting in a neurosurgical procedure introduced in 1987, involving the implantation of a medical device called a neurostimulator (sometimes referred to as a 'brain pacemaker'), which sends electrical impulses, through implanted electrodes, to specific parts of the brain (Hammond et al., 2008). The best long-term results with deep brain stimulation have been reported with targets in the periventricular/periaqueductal grey matter, or the

periventricular/periaqueductal grey matter plus thalamus and/or internal capsule (Bittar et al., 2005). Stimulation of the primary motor cortex through electrodes placed within the skull but outside the thick meningeal membrane (dura) has been used to treat pain. The level of stimulation is below that for motor stimulation. Spinal cord stimulators, use electrodes placed adjacent to, but outside the spinal cord. The overall complication rate is one-third, most commonly due to lead migration or breakage but advancements in the past decade have driven complication rates much lower (Turner et al., 2004). Another treatment is the intrathecal pumps deliver medication directly to the fluid filled (subarachnoid) space surrounding the spinal cord. Opioids alone or opioids with adjunctive medication (either a local anesthetic or clonidine) or more recently ziconotide (Lynch et al., 2006) are infused. Complications such as, serious infection (meningitis), urinary retention, hormonal disturbance and intrathecal granuloma formation have been noted with intrathecal infusion. There are no randomized studies of infusion pumps. For selected patients 50% or greater pain relief is achieved in 38% to 56% at six months but declines with the passage of time (Turner et al., 2007). These results must be viewed skeptically since placebo effects cannot be evaluated.

Innovative pharmacological treatment for neuropathic pain are being evaluated. For example, the N-methyl-D-aspartate (NMDA) receptor seems to play a major role in neuropathic pain and in the development of opioid tolerance. Dextromethorphan is an NMDA antagonist at high doses. Experiments in both animals and humans have established that NMDA antagonists such as ketamine and dextromethorphan can alleviate neuropathic pain and reverse opioid tolerance (Nelson et al., 1997). Unfortunately, only a few NMDA antagonists are clinically available and their use is limited by a very short half-life (dextromethorphan), weak activity (memantine) or unacceptable side effects (ketamine). On the other hand, opioids are increasingly recognized as important treatment options for chronic pain. They are not considered first line treatments in neuropathic pain but remain the most consistently effective class of drugs for this condition. Due to the risk of tolerance and addiction, opioids must be used only in appropriate individuals and under close medical supervision. Several opioids, particularly methadone, and ketobemidone possess NMDA antagonism in addition to their μ-opioid agonist properties. Methadone is a racemic mixture and only

the l-isomer is a potent μ-opioid agonist. The d-isomer does not have opioid agonist action and acts as an NMDA antagonist; d-methadone is analgesic in experimental models of chronic pain (Davis and Inturrisi, 1999).

In some forms of neuropathy, especially post-herpetic neuralgia, the topical application of local anesthetics such as lidocaine is reported to provide relief. A transdermal patch containing lidocaine is available commercially in some countries. In other cases repeated topical applications of capsaicin, are followed by a prolonged period of reduced skin sensibility referred to as desensitization, or nociceptor inactivation. Capsaicin not only depletes substance P but also results in a reversible degeneration of epidermal nerve fibers (Nolano et al., 1999). Nevertheless, benefits appear modest with standard (low) strength preparations, (Finnerup et al., 2007) and topical capsaicin can itself induce pain (Nolano et al., 1999).

1.3.2 Chemotherapy-induced peripheral neuropathy

Chemotherapy-induced peripheral neuropathy is the most common neurologic complication of cancer treatment, particularly with the use of platinum-derived agents, taxanes, vinca alkaloids and proteasome inhibitors which are first-line agents in the treatment of solid tumors (Bhagra and Rao, 2007). Chemotherapy regimens that utilize combination therapy may potentiate the sequela of neuropathy through agents that produce nerve damage via different mechanisms of action. Initial presentation begins with decreased vibration sense in the toes and loss of the ankle jerk reflex. Further, neuropathy may present as sensory deficits, loss of motor function and pain due to damage that occurs at multiple locations along the peripheral and central nervous system. It is estimated that up to 90% of all cancer patients treated with chemotherapy will be affected by chemotherapy-induced peripheral neuropathy (Bokhari and Sawatzky, 2009). The development of neuropathy is the most common reason for altering a platinum-based chemotherapy regimen, either by decreasing dose and frequency or by selecting a different therapeutic agent (Albers et al., 2011). Depending on the chemotherapy regimen, chemotherapy-induced painful peripheral neuropathy may self-resolve in weeks or persist for years (Smith et al., 2013). Studies on the pathophysiology of chemotherapy induced peripheral neuropathy suggest anatomical

and/or functional changes of intraepidermal nerve fibers, primary sensory neurons, CNS neurons, and involvement of glial and immune cells. Currently there is no method of preventing chemotherapy-induced peripheral neuropathy(Kim et al., 2015).

Treatment is focused mainly on the management of the clinical symptom of neuropathic pain (Kim et al., 2015). Among women with ovarian cancer, up to 51% may experience peripheral neuropathy after chemotherapy manifesting especially as numbness and tingling in the hands and feet (Ezendam et al., 2014). In the study of the addition of paclitaxel to cisplatin and doxorubicin for the treatment of advanced endometrial cancer, out of a total of 1203 patients 46.5% reported some form of peripheral neuropathy and 13.2% reported a grade 2 neuropathy, with moderate symptoms limiting instrumental activities of daily living (Bao et al., 2015). Ovarian cancer is treated with a platinum-based agent such as carboplatin and may be combined with taxanes. High-risk gestational trophoblastic neoplasia may require combination therapy including vincristine or cisplatin. Cisplatin and paclitaxel are also used in the treatment of cervical cancer (Rahaman et al., 2009). While bevacizumab alone has not been shown to cause sensory neuropathy, product information supplied by the manufacturer notes a possible increase in the rate of sensory neuropathy when used in combination with paclitaxel. Nerve injury can occur via several mechanisms during the course of treatment for cancer, and bears consideration in patients who undergo multimodal therapy. Solid tumors may cause local nerve compression depending on size and location. Worsening neuropathy in the territory of a tumor may indicate progression of disease. Surgical resection and lymph node dissection can cause immediate nerve injury due to the placement of surgical tools for retraction and stretching of tissues or delayed injury through the development of postsurgical adhesions. This may present as a non-specific visceral pain. Radiation therapy in high doses causes damage to surrounding structures which may include tumor adjacent nerves and plexuses, such as the lumbosacral plexus during irradiation of pelvic organs (Kim et al., 2015).

Due to the important role peripheral neuropathy plays in determining the course of cancer treatment, significant research has gone into understanding the mechanisms of nerve injury after exposure to different chemotherapeutic agents. Basic science research has demonstrated chemotherapy-induced nerve damage both at the level of

the peripheral and the central nervous system. The multiple areas susceptible to injury underscore the propensity towards peripheral neuropathy during the use of platinum-derived agents, taxanes, vinca alkaloids and proteasome inhibitors. Intraepidermal nerve fiber density has been found to be reduced in patients with painful sensory neuropathies, with decreased density correlating to clinical estimates of severity of pain (Boyette-Davis et al., 2011). Patients with small-fiber sensory neuropathies may have fewer objective abnormalities on clinical examination and electrodiagnostic studies (Holland et al., 1997). In the rat model, taxanes, vinca alkaloids, and platinum-based agents were found to decrease the number of intraepidermal nerve fibers of the hind paw (Siau et al., 2006). Penetration of chemotherapeutic agents into the central nervous system is relatively poor, whereas high levels have been found to accumulate within the DRG and peripheral nerves (Gregg et al., 1992). Activation of innate immunity in the DRG as a consequence of chemotherapy treatment appears to be a key early event in the initiation of CIPN (Zhang et al., 2013). The DRG of peripheral nerves are susceptible to disruption at many points, including sodium, calcium, and potassium ion channels, NMDA receptors, and mitochondria. The expression of numerous ion channels in DRG neurons are altered following chemotherapy treatment (Massey et al., 2014; Zhang and Dougherty, 2014). Activation of ion channels triggers changes in intracellular calcium that leads to the release of free radicals that subsequently induce neuropathic pain. Mitochondrial damage also increases permeability to and release of intracellular calcium, which causes activation of protein kinase C, phosphorylation of transient receptor potential vanilloid (TRPV), activation of caspases and calpains, and the release of nitric oxide and free radicals, resulting in increased excitability and cytotoxic (Massey et al., 2014). In particular, the alpha-2-delta-1 subunits of calcium channels of the DRG and dorsal horn are upregulated by paclitaxel and vincristine. Increased cytosolic calcium is present due to the release from extracellular and intracellular stores of mitochondria (Ghelardini et al., 2010; Sun and Windebank, 1996). Paclitaxel, vincristine and oxaliplatin increase the Na+ current in the DRG which accounts for the paresthesias and fasciculations associated with neuropathy (Matsumoto et al., 1984). There is decreased expression of mechano-gated and temperature-sensitive potassium channels (TREK 1, TRAAK types) in the presence of oxaliplatin (Descoeur et al., 2011). At the mitochondrial level, paclitaxel,

vincristine, cisplatin, and bortezomib cause swelling and vacuolization within the peripheral nerve axon, which increases permeability to and leakage of intracellular calcium. This in turn activates a caspase-mediated apoptotic pathway, leading to neuronal cell death (Flatters and Bennett, 2006). By increasing cytosolic calcium, oxaliplatin, paclitaxel, vincristine, and bortezomib also increase free radicals in DRG cells (Muthuraman et al., 2008). Neuronal apoptosis is also initiated by the activation of calcium-dependent proteases, calpains and caspases in DRG cells in the presence of paclitaxel, vincristine, and oxaliplatin (Boehmerle et al., 2007). The transient receptor potential vanilloid (TRPVs) act as transducers of thermal and chemical stimuli in pain-sensing neurons. Cisplatin, oxaliplatin, and paclitaxel upregulate TRPV1 and transient receptor potential (TRP) ion channels of the subgroups TRPA1 (transient receptor potential cation channel, subfamily A, member 1), TRPM8 (transient receptor potential cation channel, subfamily M (menthol), member 8) and TRPV4 in the DRG neurons causing nociceptor hyperexcitability (Anand et al., 2010). Substance P and calcitonin gene-related peptide (CGRP) are neurotransmitters that relay pain signals and these are increased in DRG neurons by paclitaxel and cisplatin (Jamieson et al., 2007). Vincristine increases the 5-hydroxytryptamine 2A receptors of 5-hydroxytryptamine on the DRG neurons and dorsal horn of the spinal cord thereby sensitizing spinal dorsal horn neurons and peripheral nociceptive fibers (Hansen et al., 2011). The platinum-based chemotherapy agents (oxaliplatin, cisplatin, carboplatin) bind DNA strands thereby inducing apoptotic cell death, particularly within the cell bodies of the DRG. Of the platinum agents, carboplatin is the least likely to produce significant neuropathy(Park et al., 2008). Cisplatin has been found to accumulate in the DRG and peripheral nerves (Meijer et al., 1999). Paclitaxel activates macrophages and microglia in the DRG, peripheral nerves and spinal cord. In addition, it has been found to stabilize microtubules and decrease epidermal nerve fiber density. With large cumulative doses, paclitaxel can also affect motor nerves (Argyriou et al., 2008).

The currently used drugs and treatments for CIPN are similar as those for other neuropathic pain types. Classes of medications utilized include anticonvulsants, antidepressants, opioids, non-opioid analgesics, and topical. First-line treatment begins with the calcium channel alpha-2-delta ligand anticonvulsants, tricyclic antidepressants (TCAs) and selective serotonin and norepinephrine reuptake inhibitors

(SSNRIs) and topical lidocaine. Opioid analgesics and tramadol represent second line therapy. Third-line therapies include other anticonvulsants and antidepressant medications, membrane stabilizer such as mexiletine, NMDA receptor antagonists, and topical agents. A multimodal approach may be the most efficacious in managing CIPN and in general neuropathic pain (Kim et al., 2015). Tramadol has some opioid effects due to its weak mu receptor activity, but also works to inhibit the reuptake of serotonin and norepinephrine. Several studies have shown that tramadol has some efficacy in treating neuropathic pain (Finnerup et al., 2005).

While some patients with chemotherapy-induced peripheral neuropathy may respond well to conservative medical management alone, others may require interventional procedures that span a range of invasiveness from superficial stimulation to permanent implantation of medical devices. Certain contraindications to invasive procedures are of greater concern in the cancer patient, such as thrombocytopenia and neutropenia. In addition, life expectancy influences the decision-making process in pursuing spinal cord stimulator or intrathecal pump implantation. It is also important to set expectations with the patient that a procedure does not obviate the need for pharmacotherapy and that the goal is pain control, not elimination of pain (Kim et al., 2015).

1.3.3 Oxaliplatin

Since the discovery of cisplatin in the ‘60s, many platinum compounds (more than 3,000 compounds) have been developed. Thirty-five of these compounds have exhibited adequate pharmacological advantages (e.g., reaching sufficiently high plasma levels not associated with common toxicities, such as renal toxicity and thrombocytopenia) (Fuertes et al., 2002). Some of them have been registered or are being considered for registration for treatment of different cancers, such as the second (carboplatin, nedaplatin, tetraplatin, and iproplatin) and third (oxaliplatin, lobaplatin, heptaplatin, satraplatin, and LA-12) generation, usually with better safety profiles (Ali et al., 2013).

Despite the efficacy of platinum analogs in cancer treatment, serious side effects, especially peripheral sensory neurotoxicity, often prevent their administration at their full efficacious doses or may considerably affect the quality of life of cancer patients

being treated with them (Cavaletti, 2014). Cisplatin was the first heavy metal used in several kinds of solid tumors, including lung, ovary, testis, bladder, head and neck, and endometrium (Mollman, 1990); most patients develop a symptomatic neuropathy (Albers et al., 2014). Second and third generations of platinum compounds have emerged in attempts to reduce the toxicity of cisplatin. Carboplatin, a second generation of platinum is used to treat ovarian, non-small cell lung, and refractory testicular cancers, was thought to be associated with a lower risk of developing neurotoxicity. However, the most recent Cochrane review comparing the toxicity of carboplatin versus cisplatin in combination with third-generation drugs for advanced non-small cell lung cancer reported an almost two times higher rate of neurotoxicity in the carboplatin group (de Castria et al., 2013). Oxaliplatin, as a widely used third-generation platinum analog approved for use in the treatment of metastatic colon cancer, is reported by the Food and Drug Administration to be responsible for more than 70% rate of symptomatic neurotoxicity with any severity (Ibrahim et al., 2004) and often leads to treatment discontinuation (Grothey and Goldberg, 2004). In other studies, approximately 80% of colorectal cancer patients treated with oxaliplatin alone or in combination with other chemotherapeutics experienced neurotoxicity (Argyriou et al., 2012b), and impairment may be permanent. Because the number of patients being treated with a neurotoxic agent is increasing, it is essential to understand the nature of such a problematic side effect. Furthermore, testing and validating available protective strategies in preclinical and clinical settings should be the next steps in overcoming platinum-induced peripheral neurotoxicity(Avan et al., 2015).

Platinum drugs are usually given in combination with other chemotherapy drugs and/or radiation that may be neurotoxic in their own right. Early presentation of peripheral neurotoxicity can be with numbness, tingling, or paresthesia in fingers and/or toes, a decreased distal vibratory sensitivity, and/or loss of ankle jerks. Moreover, prolonged treatment may also affect proprioception, which may result in ataxic gait. Oxaliplatin and cisplatin are the two most commonly used neurotoxic platinum agents. Platinum-induced peripheral neurotoxicity can present as two clinically distinct syndromes. The acute transient paresthesia in the distal extremities, which is only commonly seen with oxaliplatin, usually occurs within the early phase of drug administration, whereas the chronic cumulative sensory neuropathy causes

more persistent clinical impairments (Argyriou et al., 2012a). The latter deteriorates with cumulative doses, followed by "coasting," wherein symptoms worsen even months after treatment withdrawal. Furthermore, patients can develop Lhermitte's syndrome, which is a shock-like sensation of paresthesia radiating from the neck to the feet triggered by neck flexion. This phenomenon indicates the involvement of the centripetal branch of the sensory pathway within the spinal cord (Cavaletti et al., 2011). Neuropathy can also become irreversible. In a prospective multicenter study, Argyriou and collaborators reported that oxaliplatin can result in an acute and chronic rate of neuropathy in 85% (169 patients of 200) and 73% (145 patients of 200) of patients, respectively (Argyriou et al., 2013).

The clinical diagnosis of platinum-induced neuropathy is generally not very difficult. Nerve biopsies and neurophysiologic assessments are helpful for the examination of pathological and functional nerve damage (e.g., demyelinating versus axonal pathology; abnormalities in nerve conduction studies, somatosensory evoked potentials, magnetic resonance imaging, threshold tracking techniques, and quantitative sensory testing) (Verstappen et al., 2003). Objective electromyography assessment of motor nerve excitability is a sensitive and specific endpoint of acute oxaliplatin-induced motor nerve hyperexcitability, which has the advantage of being widely available (Wilson et al., 2002). Additionally, the threshold tracking technique is used to assess axonal excitability (Krishnan et al., 2006). This technique allows the detection of sensory axonal dysfunction before clinical symptoms and can be used as a predictive marker for nerve dysfunction (Park et al., 2009). Chemotherapy-induced peripheral neurotoxicity is typically a multidisciplinary medical issue, leading to different terminology, measurement, clinical evaluation, and grading, precluding the reliability of neurological assessment. However, standardization is improving. The Functional Assessment of Cancer Therapy/Gynecologic Oncology Group-Neurotoxicity Scale, the FACT-Taxane scales, the Patient Neurotoxicity Questionnaire, European Organization for Research and Treatment of Cancer (EORTC) quality of life questionnaire [QLQ] to assess chemotherapy-induced peripheral neuropathy, and the EORTC QLQ C30 questionnaire are scoring systems that have been used for neurotoxicity assessment to quantify the impact of chemotherapy-induced neurotoxicity on patients' quality of life. Among the

questionnaires, the EORTC questionnaires are widely used nowadays (Alberti et al., 2014). Among different common toxicity criteria scales that are used for peripheral neurotoxicity assessment, the one developed by the Eastern Cooperative Oncology Group and National Cancer Institute (NCI-CTC) is most widely used. (Avan et al., 2015).

The pathophysiology of platinum-induced peripheral neurotoxicity is not completely elucidated. Based on available data, platinum compounds may actively enter the tumor and normal cells through organic cation transporters (Sprowl et al., 2013), organic cation/ carnitine transporters, and some metal transporters, such as the copper transporters (Liu et al., 2013). Platinum compounds can be excreted via platinum efflux transporters (ATP7A, ATP7B, and MRP2) (Yamasaki et al., 2011). The platinum adducts are formed intracellularly because of a hydrolysis process, resulting in interstrand cross-links, intrastrand cross-links and/or DNA-protein cross-links with platinum, affecting DNA synthesis in cancer cells and mediating apoptosis (McDonald et al., 2005). Extensive DNA repair is considered as a major mechanism of chemotherapy resistance, but efficient DNA repair can possibly prevent development of neurotoxicity. In dividing tumor cells, the formation of DNA adducts is supposed to cause growth inhibition and cell death, hence eliminating the tumor cells (Avan et al., 2015). Platinum products accumulate in the DRG and in peripheral neurons. Because these cells are postmitotic and not dividing, the formation of DNA adducts is not lethal, although the extent of DNA cross-links in DRG neurons at a specific cumulative dose strongly correlates with the degree of neurotoxicity (Dzagnidze et al., 2007). Platinum adducts probably cause axonal changes secondary to the neuronal damage, whereas brain and spinal cord are to some extent protected by the blood-brain barrier (BBB). However, there are data showing that cisplatin crosses the BBB and can accumulate when repeated dosages are given. This can cause demyelination and vacuolar changes in the white matter (Olivi et al., 1993).

As for other CIPN oxidative stress and mitochondrial dysfunction could be regarded as probable etiology of the apoptosis. Podratz and collaborators showed that cisplatin might inhibit mitochondrial DNA replication and cause mitochondrial vacuolization and degradation in DRG neurons *in vitro* and *in vivo* (Podratz et al., 2011). On the other hand, alteration in the expression of sodium, potassium, calcium and other ion

channels are well described following oxaliplatin treatment (Avan et al., 2015; Descoeur et al., 2011). These events can, to some extent, explain the mechanism of the neurotoxic effect of platinum compounds.

There are some promising results favoring the ability of neuroprotective agents to reduce the rate of subsequent neurotoxicity induced by platinum analogs. However, the most recent update of the Cochrane review on chemoneuroprotective agents found insufficient data to conclude that any of the available chemoprotective agents is sufficiently effective in preventing or limiting the neurotoxicity of platinum drugs (Avan et al., 2015). Albers and collaborators reviewed 29 randomized controlled trials (RCTs) or quasi-RCTs, in which 2,906 participants received chemotherapy with cisplatin or related compounds (Albers et al., 2014). Patients were also evaluated for quantitative sensory testing (primary outcome) or other measures including nerve conduction or neurological impairment rating using validated scales (secondary outcomes) before and 6 months after completing chemotherapy. Likewise, the most recent ASCO Clinical Practice Guideline based on a systematic review on 48 RCTs, including 35 RCTs on platinum-induced peripheral sensory neurotoxicity, did not recommend any established agent for the prevention of platinum-induced peripheral neurotoxicity. Only for the treatment of existing oxaliplatin neuropathy, they advised duloxetine, for which intermediate strength of evidence is present, considering the balance between benefit and harm (Hershman et al., 2014). Altogether, no neuroprotective strategy can yet be recommended for prevention and treatment of platinum induced neurotoxicity. There is a genetic diversity between patients, leading to differences in drug response including the side effects; hence a neuropathy preventive strategy should be individualized for each patient. A pharmacogenetic approach might be useful in understanding the cause of peripheral neurotoxicity and tailoring the most suitable chemotherapy for each patient. A genome-wide pharmacogenomics approach may also be useful in identifying novel polymorphism predictors of severe platinum induced peripheral neurotoxicity that may be used in personalized chemotherapy. However, it is highly recommended that the positive and negative effects of the antineoplastic agents be studied in detail in preclinical settings, before implementation in clinical practice. In particular, the central nervous system of animals can be used to quantify the effects of platinated compounds on neurons that

corroborate clinical data and suggest them as suitable models for studying possible neurotoxicity of platinum agents. Some in vitro models can also be used to investigate morphological parameters affected by platinum compounds (Ceresa et al., 2014). These models enable measuring the effect of the drugs on neurons along with testing the neurogenic potential of neuroprotective compounds (Avan et al., 2015).

2. Hyperpolarization-activated cyclic nucleotide gated channels

The hyperpolarization-activated current (Ih) was first described in sino-atrial node cells and later identified in different types of neurons (Noma and Irisawa, 1976). Because of its unique properties, especially the activation upon hyperpolarization of the membrane potential, it was termed If (f for funny).

The ion channels underlying Ih have been discovered about a decade ago and, because of their complex dual gating mode, these proteins were termed hyperpolarization-activated cyclic nucleotide gated (HCN) channels.

In mammals, four different genes encoding HCN isoforms (HCN1-4) have been discovered, each isoform forming channels with significantly different physiological properties (Santoro et al., 1998). Currents obtained after heterologous expression of HCN1-4 channels cDNA reveal the principal features of native Ih, confirming that HCN channels indeed represent the molecular correlate of Ih. Different HCN isoforms have been found in the same cells and their co-assembly has been suggested using electrophysiological analyses (Chen et al., 2001).

Ih contributes to a wide range of physiological functions, including the determination of resting membrane potential (RMP), generation of neuronal oscillation, and regulation of dendritic integration and synaptic transmission, and is implicated in multiple physiological processes, such as sleep and arousal, learning and memory and perception.

2.1 HCN channels

Each HCN subunit is composed of six alpha-helical segments (referred to as S1-S6) forming a transmembrane channel core. The region forming the ion-conducting pore

loop is between S5 and S6, while the ion selectivity filter is constituted by the pore region carrying the GYG motif between S5 and S6. The S4 segment carries nine arginine or lysine regularly spaced at every third position (Chen et al., 2000); its resulting positive charge confers to it the role of voltage-sensitive domain. All the voltage-dependent members of the pore-loop cation channel superfamily present positively charged S4 segments (Yu and Catterall, 2004), but while inward movement of S4 charges leads to the closure of depolarization-activated channels, in HCN channel it triggers their opening. Following, S6 is a region called "cAMP-sensing domain" (CSD), formed by a cyclic nucleotide binding domain (CNBD) and a carboxyl terminus segment termed C-linker. The CSD is needed in order to elicit a cAMP-induced positive shift of the voltage-dependent activation of HCN channels.

The four subtypes of HCN channels exhibit distinct cAMP-sensitivity and activation kinetics: HCN1 channels show the more positive threshold for activation, the fastest activation kinetics, and the lowest sensitivity to cAMP, while HCN4 channels are slowly gating and strongly sensitive to cAMP. HCN2 and HCN3 have intermediate properties (Baruscotti et al., 2005); Santoro et al., 1998).

2.1.1 Tissue and subcellular expression

Studies at mRNA and protein levels have demonstrated distinct expression patterns in the central nervous system (CNS) of the four HCN subunits (Notomi and Shigemoto, 2004).

HCN1 is mainly expressed in neocortex, hippocampus, cerebellar cortex and brain stem. HCN2 subunit is widespread throughout the brain with the highest expression in the thalamus and brainstem nuclei (Santoro et al., 2000). HCN3 distributes sparsely with the lowest expression level in CNS, but is present in olfactory bulb, hypothalamus and SNc. The distributed pattern of HCN4 is complimentary to HCN1, and HCN4 is selectively expressed in various thalamic nuclei and distinct neuronal populations of the basal ganglia and habenular complex (Moosmang et al., 1999); Santoro et al., 2000). HCN channels have also been identified in peripheral neurons, such as the dorsal root and trigeminal ganglion neurons. All four HCN subunits and Ih have been identified in the dorsal root ganglion, with HCN1 exhibiting the highest expression (Chaplan et al., 2003); Moosmang et al., 2001), and the majority of trigeminal ganglion

neurons were immune-positive for HCN1, HCN2 and HCN3 (Wells et al., 2007). In SNc DA neurons, only the mRNA of HCN2, HCN3 and HCN4 were detected by using qualitative single-cell RT-mPCR or in situ hybridization. In accordance with the lack of HCN1 subunit, native Ih recorded in SNc DA neurons show larger activation time constants and bigger cAMP sensitivity than their counterparts in hippocampal pyramidal neurons (Franz et al., 2000) suggesting that in this area Ih is mainly mediated by HCN2-HCN4 subunits.

The subcellular localization of HCN channels can be neuron-type-specific and can influence the effects that they exert on neuronal properties and activity. For instance, in neocortical and CA1 hippocampal pyramidal neurons, HCN1 channels are concentrated in the apical dendrites, and channel density is much higher in the distal compared with the proximal dendritic span (Lörincz et al., 2002). This gradient has been shown to contribute to normalizing dendritic inputs arriving at different locations along the dendrite (Magee, 1998).

In the interneurons of medial septum, hippocampus and cerebellum, all the HCN isoforms except for the HCN3 are expressed at somatic and axonal regions, where they regulate membrane properties and influence neurotransmitters release. In the entorhinal cortex, localization of HCN1 channels is prevalent in the axon terminal during development and their presynaptic expression and functions disappear with maturation. (Bender et al., 2007).

Interestingly, patterns of distribution of HCN1 channels have been recently shown to depend on neuronal network activity: e.g. after the elimination of synchronized neuronal input to the distal dendrites of CA1 pyramidal neurons, the gradient of HCN1 channel distribution was abolished (Shin and Chetkovich, 2007).

2.2 Hyperpolarization- activated current (Ih)

Ih is a mixed cationic current carried by Na^+ and K^+ with permeability ratios of about 1:4; however, recent findings support the evidence of a small but significant Ca^{2+} permeability. Given its reversal potential around −20 mV and −30 mV at physiological

ionic conditions (Biel et al., 2009), Ih is inwardly directed at rest and depolarizes the membrane potential.

Unlike most voltage-gated currents, is activated by hyperpolarizing voltage steps to potentials negative to −60 mV, near the RMP, and does not display voltage-dependent inactivation. Although Na^+ constitutes the major inward cation current in HCN channels at physiological membrane potentials, the Ih current amplitude depends on the extracellular K^+ concentration (Wollmuth and Hille, 1992).

Upon activation of Ih , two kinetic components can be distinguished: a minor instantaneous current (IINS) fully activated within a few milliseconds, and the major slowly developing component (ISS), which reaches the steady-state level under fully activating conditions in a range of tens of milliseconds to several seconds. To date the ionic nature of IINS is not clear and is generally considered as a leak conductance or an experimental artifact (Macri and Accili, 2004; Macri et al., 2002). In general HCN channels activate quite slowly with time constants and the ISS can be empirically described by either a single (Womble and Moises, 1993) (see formula 2.2) or double exponential function (see equation 2.1), where Ih_t is the amplitude of the current at time *t*, *C* is a constant, A_1 and A_2 reflect the amplitude coefficients of the fast (τ_1) and slow (τ_2) time constants, respectively. (van Ginneken and Giles, 1991).

$$\mathrm{Iht} = A1 \times e^{-t/\tau 1} + A2 \times e^{-t/\tau 2} + C \qquad (2.1)$$

The diversity of time constants probably results from an interplay of several factors: in addition to the intrinsic activation properties of HCN channel isoforms, cellular microenvironment (e.g. auxiliary subunits, concentration of cellular factors, etc.) can affect Ih properties as well as experimental conditions (e.g. pH, temperature, ionic composition of solutions, etc.).

The voltage-dependence of Ih activation can be assessed by tail current activation curves, in which the amplitude of the tail current upon return to a fixed holding potential is plotted against the hyperpolarizing potential step used to activate the current. These activation curves show a typical sigmoidal profile and can be well fitted

by Boltzmann function (see equation 2.2), providing estimation of the half-maximal activation potential ($V_{1/2}$) and steepness factor (*k*).

$$I_h = \frac{I_{h_{max}}}{1 + \exp\left(\frac{V - V_{1/2}}{k}\right)} \quad (2.2)$$

2.2.1 Regulation

External temperature can modulate Ih current by shifting the midpoint of voltage-dependent activation curve towards more depolarized potentials and reducing Ih time constants (Watts et al., 1996); thus performing experiments with a constant temperature is fundamental when investigating Ih.

Another positive Ih modulator is phosphatidylinositol 4,5-bisphosphate (PIP_2), which positively shifts the activation curve of cloned HCN2 channels, by 20-30 mV (Zolles et al., 2006). PIP_2 effect is largely cAMP-independent and prevents the hyperpolarized shift normally observed in excised patches (Chen et al., 2001; DiFrancesco et al., 1986), meaning that endogenous PIP_2 levels counterbalance the opposing action of corresponding kinases and phosphatases on native Ih current voltage dependence (Zolles et al., 2006).

In addition it has been shown that in hippocampal neurons, the inhibition p38 mitogen associated protein kinase (MAPK) negatively shifts the activation curve by 25 mV, whereas its activation induced a positive shift by 11 mV (Poolos et al., 2006).

2.2.2 Pharmacology

The common characteristic of all Ih blockers is their lack of full selectivity for HCN channels; in addition, there are no isoform-specific compounds allowing identification of subunit-specific roles in various tissues. Like K^+ channels, HCN channels are almost completely blocked by low millimolar concentrations of Cs, however, in contrast to inward rectifier K^+ currents, Ih is insensitive to millimolar concentrations of external

Ba^{2+} and tetraethylammonium (TEA). Ih is also insensitive to 4-Aminopyridine (4-AP), a blocker of voltage-gated K^+ channels (Ludwig et al., 1998).

A number of organic blockers have been described to inhibits HCN channels; among them, the most widely used is a bradycardic one termed ZD7288 (originally named ICI 7288)(Briggs et al., 1994). ZD7288 blocks Ih at concentrations between 10 µm to 100 µm (Gasparini and DiFrancesco, 1997) and exhibits slow kinetics, ranging in the order of minutes; in addition is poorly reversible and its Ih inhibition is not use dependent. It has been suggested that the localization of ZD7288 binding site is near the intracellular portion of the HCN channel pore as confirmed by a specific analysis carried on HCN1 expressing HEK293 cells, where it was demonstrated that, to exert its action, ZD7288 needs the channel to be open and is trapped by its closing. Ivabradine is the only organic Ih blocker used in therapy, in particular for symptomatic treatment of chronic stable angina pectoris. It reduces heart rate via inhibition of HCN4 channels, which role in regulating pacemaker activity in the sinoatrial node cells is crucial. Ivabradine blocks HCN channels in a use-dependent manner by occupying a cavity below the channel pore and shows an IC_{50} between 2 and 3 µm (Bucchi et al., 2013).

Finally, QX-314, the quaternary derivative of lidocaine normally employed to abolish voltage-activated Na channels, it's reported to block Ih in CA1 pyramidal cells (Perkins and Wong, 1995).

2.3 Physiological roles of Ih in neural function

2.3.1. I_h and spontaneous activity

Given it activation near RMP and its non-activating properties, Ih exerts a depolarizing action on neural resting properties in many different cell types (Pape, 1996). Activation of Ih around rests stabilizes membrane potential against

hyperpolarization (Nolan et al., 2003), while its deactivation antagonizes membrane depolarization (Magee, 1999).

Interactions between HCN channels and inwardly rectifying potassium channels (KIR) in pyramidal cell dendrites maintain Ih sufficiently high for its control of temporal summation (Day et al., 2005).

In rat interneurons of the stratum oriens/alveus of hippocampus, Ih inhibition causes a reduction in action potential frequency and a membrane hyperpolarization concomitant with an increased input resistance in current-clamp recordings (Maccaferri and McBain, 1996). Therefore, Ih can affect the excitability of these neurons in two ways: reducing the probability of cell firing induced by an excitatory stimulus and increasing the voltage change after a given amount of injected current because of the increased membrane input resistance.

In contrast, in rat cerebellar Purkinje neurons, Ih does not control the frequency of action potentials but rather maintains the membrane potential within a range where the inward sodium current operates. Consequently, tonic firing could persist even when challenged by several spontaneous inhibitory postsynaptic inputs (Häusser and Clark, 1997).

2.3.2. I_h role in synaptic transmission

It has been demonstrated that Ih increases excitatory synaptic release in a "non-ionic" way via a pathway involving actin depolymerization. These findings suggest that HCN channels might modulate synaptic release by triggering processes altering the cytoskeleton or modifying the terminal resistance or RMP, as demonstrated in cortical neurons postsynaptic dendrites. In addition to their dendritic localization, HCN channels are also present on certain axons and synaptic terminals suggesting that Ih influences synaptic transmission. It has been shown that presynaptic Ih affects inhibitory synaptic transmission in rodent cerebellum, hippocampus, but the underlying mechanism is still unknown (Huang et al., 2011).

Recently it has been demonstrated that in entorhinal cortical layer III pyramidal neurons, HCN1 subunits colocalize with Cav3.2 T-type Ca^{2+} channel on synaptic terminals and depolarize RMP, restricting Ca^{2+} entry via T-type Ca^{2+} channel activity and preventing glutamate release. Ih driven alteration of T-type Ca^{2+} channel activity

has been also observed in hippocampal dendrites (Huang et al., 2011); therefore, this might be a common mechanism by which these channels affect neuronal excitability.

2.3.3. I_h in dendritic integration

Great part of synaptic inputs are located within dendritic arbors, where inhibitory and excitatory signals are blended together to form a coherent output response. While synaptic inputs are widely distributed across complicated dendritic arbors, the action potential output is confined in a relatively localized region of the soma or in the proximal axon (Colbert and Johnston, 1996). Amplitude and temporal characteristics of signals can differ at the final integration site depending on variation in their synaptic distance, meaning that the effect of any given synapse on output depends upon its location (Mainen and Sejnowski, 1996). Under passive conditions, the amplitude and kinetics of a given excitatory postsynaptic potential (EPSP) vary inversely with the distance of the synapse from the soma; thus, EPSPs from distal synapse will be smaller and slower than their proximal counterparts (Magee, 2000).

Location-dependent synaptic variability could interfere with a neuron's ability to accurately determinate the total amount of incoming synaptic activity or increase the variability of action potential discharge, therefore, mechanisms for contrasting the dependence of synaptic summation on input location might be very advantageous. Ih seems to be well suited to influencing the integration of subthreshold synaptic input: during synaptic activity, Ih deactivation by synaptic depolarization produces a hyperpolarizing current that tends to counterbalance the location-dependent kinetic (but not amplitude) filtering effects for a wide range of spatiotemporal input patterns (Magee, 1999).

In neocortical and CA1 pyramidal neurons, HCN channels density is distributed as a gradient, reaching in dendrites a density nearly sevenfold bigger than the one observed in the soma, and therefore producing a sustained hyperpolarization current

which amplitude increases with the distance from in neurons the soma (Pettit and Augustine, 2000).

This hyperpolarization gradient permits primarily proximal input to produce the same temporal output pattern as distal input, allowing the generation of a neuron's response largely reflecting the temporal pattern of the synaptic input.

With Ih blocked, neurons fires indiscriminately during both coincident and temporally dispersed input; therefore a spatially normalized temporal summation allows a neuron to lower the variability of action potential firing, improving the synchrony of neuronal population activity (Jaffe and Carnevale, 1999).

3. Role of Ih in pain

Ih was first discovered in neurons by Mayer and Westbrook in a study of mechanisms of anomalous rectification in the embryonic mouse dorsal root ganglion (DRG) (Mayer and Westbrook, 1983). They described the presence of a time- and voltage-dependent conductance activated by membrane hyperpolarization with strikingly similar characteristics to the "pacemaker current" If identified in sinoatrial node cells a few years before (Yanagihara and Irisawa, 1980). Later it was shown that expression of Ih was most prominent in large and medium sized neurons, whereas only half of small sized DRG neurons displayed a functional Ih current (Scroggs et al., 1994). Among the different isoforms, HCN1 and HCN2 were predominantly expressed in dorsal root ganglions, while expression of HCN3 and HCN4 was low or undetectable (Acosta et al., 2012). HCN2 was more frequently found in small sized neurons, whereas HCN1 was the predominant subunit in large neurons (Schnorr et al., 2014). These data are consistent with the electrophysiological findings of a faster activating and less cAMP-sensitive Ih in large and medium sized DRG neurons as compared to the characteristics of the current in small diameter neurons (Gao et al., 2012). The available HCN knockout studies largely confirm this pattern of HCN isoform expression in the different neuronal subtypes of the DRG. The deletion of HCN1 abolished Ih in most large neurons but left unaffected the slowly activating cAMP-sensitive Ih, preferably present in smaller DRG neurons (Momin et al., 2008). In contrast, this component was eliminated by (ubiquitous) deletion of HCN2 (Emery et al., 2011). Despite the relatively high and broad expression in sensory neurons, the

physiological role of Ih for sensory function is unknown. The results of a huge number of animal studies analyzing physiological sensation *in vivo* by the use of HCN blockers or mouse mutants argue against an obvious function of Ih in healthy sensory neurons. In addition, the wide clinical use of the Ih blocker ivabradine for the treatment of stable angina and heart failure is not associated with peripheral sensory side effects such as dysesthesias and paresthesias. It seems that HCN channel function in the peripheral sensory system is limited to pathological pain conditions, which might make these channels an attractive target for the treatment of pain disorders. Several studies reported enhanced HCN channel expression and/or Ih activity in the peripheral pain pathway following neuronal damage (Chaplan et al., 2003; Jiang et al., 2008b; Yao et al., 2003) or inflammation (Acosta et al., 2012; Papp et al., 2010; Schnorr et al., 2014; Weng et al., 2012). These observations have raised the hypothesis that nociceptor hyperexcitability, which is associated with hyperalgesia and allodynia, is attributed to an increased activity of Ih in the pain sensing pathway (Herrmann et al., 2015). This is plausible because HCN channels conduct an excitatory mixed inward current, which is typically activated near the neuronal resting membrane potential. A pronounced HCN activity in sensory neurons following nerve injury or inflammation may shift membrane potential to more depolarized values. This lowers the activation threshold of nociceptors and facilitates spontaneous and/or neuronal repetitive activity in line with the increased sensitization to painful stimuli. Such an increased functional importance of Ih may mechanistically be attributed to enhanced gene expression (Descoeur et al., 2011; Papp et al., 2010; Schnorr et al., 2014), PIP2 interaction (Pian et al., 2007), channel phosphorylation (Cheng and Zhou, 2013) or to elevated levels of cAMP typically triggered by inflammatory substances such as PGE2 (prostaglandin E2), serotonin and substance P (Jafri and Weinreich, 1998).

A possible involvement of peripheral HCN channels in inflammatory pain conditions has been tested in several animal models using Ih channel blockers or HCN knockouts, with however surprisingly different results depending on the inflammatory agent and behavioral readout used. A significant analgesic effect of ZD7288 was first seen in the carrageenan inflammation model testing heat hyperalgesia in rats (Dunlop et al., 2009). Later it was shown that HCN2 channels expressed in a subpopulation of small nociceptive neurons were predominantly responsible for this heat hyperalgesia,

since the pronounced nociceptive behavior was drastically reduced in conditional HCN2 knockouts after carrageenan or PGE2-mediated inflammation (Emery et al., 2011). Interestingly, PGE2-mediated mechanical hypersensitivity was not affected by HCN2 gene deletion or a pan-HCN channel block (Herrmann et al., 2015). Peripheral HCN2 channels control the acute phase of neuronal hypersensitivity as long as the inflammatory processes activate signaling transduction pathways, which cause an increase of cAMP in pain-sensing neurons. This fits well with observations made in isolated DRG neurons where cAMP shifted the resting membrane potential to depolarized values and increased action potential firing, which however was not present in neurons isolated from HCN2 knockouts or in the presence of HCN channel blockers (Young et al., 2014). On the other hand, this implies that inflammatory compounds, which elicit acute neuronal sensitization without elevating cAMP in nociceptive terminals, may act via an HCN independent mechanism (Herrmann et al., 2015). The concept of increased cAMP levels as a condition for HCN-mediated sensitization applies to acute inflammatory states, but may not be relevant for chronic inflammatory pain conditions where transcriptional regulatory processes are more important. This fits well to the observed up-regulation of HCN2 protein expression in small DRG neurons and in the spinal dorsal horn after chronic inflammation following peripheral injection of complete Freunds adjuvant (CFA) (Antal et al., 2004; Papp et al., 2010; Schnorr et al., 2014). It was shown, that the enhanced Ih contributes to neuronal sensitization since deletion of HCN2 as well as administration of ZD7288 reversed tactile hypersensitivity in CFA-inflamed animals (Schnorr et al., 2014). The neuronal site of HCN action was studied by analyzing pain behavior in controls and conditional HCN2 mutants (snsHCN2KO) after local administration of ZD7288. The region-specific block at peripheral nociceptors as well as at spinal terminals reduced mechanically evoked pain in controls, but was without any effect in snsHCN2KOs. This suggests that up-regulation of HCN2 lowers the nociceptor threshold as well as facilitates neuronal transmission in the spinal cord. Surprisingly it appears that only tactile hyperexcitability is determined by nociceptive HCN channels, since HCN2 deletion or HCN channel block showed no change in heat hyperalgesia in chronic inflammation models (Schnorr et al., 2014). These results suggest that mechanical and

thermal sensitization are conveyed by distinct neuronal pathways in chronic inflammatory conditions (Cavanaugh et al., 2009; Herrmann et al., 2015).

3.1 HCN channels in neuropathic pain

A significant involvement of Ih to tactile allodynia and thermal hyperalgesia was first demonstrated by studying the analgesic effect of the unselective HCN channel blocker ZD7288 in various neuropathic pain models including the CCI model (chronic constriction injury), the Chung model (L5/6 spinal nerve ligation) and the Seltzer model (partial sciatic nerve injury) (Dalle and Eisenach, 2005; Jiang et al., 2008b; Takasu et al., 2010). In all these models, ZD7288 caused a strong reversal of pain behavior in response to both mechanical and thermal stimulation. HCN channels are widely expressed throughout the peripheral pain pathway. They were found at peripheral and spinal terminals, in the perikaryon as well as along the axon of the DRG neuron (Papp et al., 2010; Papp et al., 2006). An important site for HCN-mediated hyperexcitability appears to be in the skin and along the axon, since intraplantar as well as perineural administration of ZD7288 significantly reduced neuropathic pain behavior (Dalle and Eisenach, 2005). It is not clear if presynaptic HCN channels are also involved in the facilitated spinal transmission as a consequence of peripheral nerve injury, because intrathecal administration of ZD7288 produced ambiguous results (Takasu et al., 2010) and nonspecific drug effects were suggested (Chevaleyre and Castillo, 2002). Experiments with genetically engineered HCN mutants confirmed the substantial participation of Ih to neuropathic pain and suggested a pivotal role for HCN2 (Schnorr et al., 2014). Emery and collaborators demonstrated that conditional deletion of HCN2 abolished pain behavior in the CCI model (Emery et al., 2012). That was largely confirm in a different model of neuropathy using a virtually identical HCN2 mutant (snsHCN2KO) (Herrmann et al., 2015).

3.1.1 HCN channels role in CIPN

Nowadays, very few studies consider the HCN channels role in CIPN. Recently Haijun Zhang and collaborators demonstrated an increased expression of HCN1 in DRG neurons in a rat model of Paclitaxel-induced peripheral neuropathy. They

observed also an increased frequency of spontaneous discharging neurons in both myelinated and unmyelinated neurons. The hyperpolarization-activated current (Ih) mediated by HCN1 may facilitate the rise of spontaneous activity in these neurons (Zhang and Dougherty, 2014). Furthermore, Juliette Descoeur and co-authors observed a significant increase in HCN1 mRNA levels in DRG from oxaliplatin treated mice. Moreover, they observed that ivabradine could exert analgesic effect on cold allodynia but not on mechanical hyperalgesia (Descour et al. 2011). These two example provide evidence of a prominent role for HCN channel in chemotherapy-induced neuropathy.

3.2 HCN channels blockers and pain

So far a number of HCN blockers have been discovered, including Cs+, ZD7288, alinidine (ST-567), zatabradine (UL-FS49), DK-AH 268 and ivabradine (S16257) (Robinson and Siegelbaum, 2003). Inhibition of Ih by these blockers can reduce the rate of heart beat, hence Ih blockers are also called bradycardics (Bucchi et al., 2007). ZD7288 is the most widely used in the study of Ih due to its high specificity and commercial availability. Therefore, most of our knowledge about the functions of Ih, including its role in pain, has been obtained by using ZD7288. However, some of these findings are recently questioned as a result of the discovery of the nonspecific effects of ZD7288. For example, T-type calcium channels were found to be inhibited by relatively higher concentration of ZD7288 in the mouse spermatogenic cells (Felix et al., 2003). It was considered that Ih and it cooperated in the peacemaking process in both SAN cells and thalamic relay neurons (Jiang et al., 2008a). It would be very hard to differentiate the role of these two channels by ZD7288. However, there are two clues that might be helpful in clarifying this issue. First, the inhibition of Ih by ZD7288 is much more effective than that of T-type calcium channels (IC50 was 2 μM and 100 μM for inhibition of Ih and IT respectively). It is reasonable to assume that ZD7288 will preferentially inhibit Ih rather than IT. Second, the effect of ZD7288 on Ih is irreversible, in contrast, IT showed partial recovery after washout. In view of the

sustained suppression of ectopic discharges by low dose of ZD7288, it is more likely that ZD7288 targets at Ih(Jiang et al., 2008a).

Ivabradine is the first and to date the only HCN blocker introduced into clinical therapy. In isolated sinoatrial node cells, ivabradine blocks HCN pacemaker currents in the low micromolar range with minimal or no off-target effects. Channel block is accomplished from the cytoplasmic side with a strong preference for the open channel state resulting in use-dependence characteristics. This may minimize the risk for severe bradycardia and improve efficacy during elevated heart rates. At therapeutic concentrations, ivabradine exclusively reduces heart rate without affecting myocardial contractility or intracardiac conduction. Since an elevated heart rate is thought to be an independent cardiovascular risk factor, drugs causing a selective reduction in heart rate should constitute an interesting therapeutic option.

Very recently, HCN1, 2 and 4 transgenic mice have been successfully established and widely used in understanding various physiological and pathological functions of Ih in cardiovascular and nervous systems (Jiang et al., 2008a).

A progress in the therapeutic use of HCN channel blockers could be achieved with the development of subtype-selective drugs. Typical side effects of ivabradine are phosphenes (spontaneous visual sensations), which are most probably caused by the block of HCN1 in retinal photoreceptors (Cervetto et al., 2007). A subtype-selective HCN4 blocker should be effective in lowering heart rate without this visual side. A selective HCN2 blocker might also be promising, particularly for the treatment of chronic pain conditions including neuropathy and inflammation. This is of particular interest since the available therapies for chronic pain states are often unsatisfactory (Herrmann et al., 2015).

4. G-protein coupled receptor 35

GPR35 is a poorly characterized 7-transmembrane domain GPCR that transmits function via interaction with Gαi/o, G13, and βarrestin (Divorty et al., 2015; Shore and Reggio, 2015). In terms of sequence similarity, GPR35 is related to the purinergic receptor LPA4 (32%), the hydroxycarboxylic acid binding receptors HCA2 and HCA3 (30%), and the cannabinoid and lysophosphatidylinositol-binding GPR55 receptor

(30%) (O'Dowd et al., 1998). As a consequence of the ligand-binding properties and shared sequence identity with GPR55, various groups have focused on GPR35 as a putative lysophosphatidic acid-sensing GPCR (Zhao and Abood, 2013). This is of interest to further investigate experimentally, although at present it is difficult to draw any conclusions based on the original findings (Oka et al., 2010). GPR35 is activated by high concentrations of kynurenic acid, a well-studied metabolite of tryptophan (Mackenzie and Milligan, 2015). Kynurenic acid is clearly neuroactive and produces a broad range of effects in the central nervous system (CNS). However, many of these effects can be attributed to blockade of ionotropic receptors for the excitatory amino acid glutamate. Specific challenges in exploring the roles of GPR35 in the CNS relate to the low potency of kynurenic acid at both rodent, and particularly the human, orthologues of the receptor (Mackenzie and Milligan, 2015). Furthermore, many ligands with activity at GPR35 have been reported to display modest potency and to have a range of non-GPR35 mediated effects. Although antagonists from two distinct chemical classes have been identified, at least in transfected cell systems these appear to display exquisite selectivity for human GPR35 and lack significant affinity at either mouse or rat GPR35 (Jenkins et al., 2012). Moreover, a line of GPR35 knock-out mice has been generated and reported (Min et al., 2010), but these have not been employed widely and, currently, no information on the elimination of expression of GPR35 on effects of kynurenic acid in cells or issue from the CNS has been released into the public domain (Mackenzie and Milligan, 2015).

4.1 GRP35 expression and physiology

Interest in GPR35 in the context of neuropharmacology is relatively recent. In part, this may stem from initial studies suggesting that GPR35 was not expressed to a significant level in human or rat brain (Wang et al., 2006). These studies employed RNA from broad brain regions and/or relatively insensitive detection methods. Subsequently, however, GPR35 expression has been identified within discrete regions of the CNS and peripheral nervous system, including the caudate nucleus in human, the medulla oblongata, hippocampus, spinal cord and dorsal root ganglia (DRG) of mouse (Cosi et al., 2011), and the DRG, spinal cord, hippocampus and cerebrum of rat

(Alkondon et al., 2015; Berlinguer-Palmini et al., 2013). Moreover, substantial levels of GPR35 mRNA recorded in other tissues, including high levels in immune and gastrointestinal tissue (Yang et al., 2010), and lower levels in heart, lung and skeletal muscle (Min et al., 2010; Taniguchi et al., 2006) had focused attention on these tissues, and diseases associated with their dysregulation, as being more appropriate to explore the function and therapeutic potential of GPR35(Milligan, 2011). Studies that detect mRNA corresponding to GPR35 are consistent with localized CNS expression, with a number of reports expanding this to immunodetection (Cosi et al., 2011; Ohshiro et al., 2008). Although such studies are of vital importance to confirm expression, concerns about the specificity of staining with many anti-GPCR antisera remain widespread (Michel et al., 2009) and controls employing tissue from knock-out animals are currently lacking to adequately validate antibody/antisera specificity.

GPR35 was first identified in genomic DNA through homology cloning using degenerate oligonucleotide primer sequences based on the transmembrane sequence of GPR1 (O'Dowd et al., 1998). Human GPR35, situated at chromosomal locus 2q37.3, encodes two alternatively spliced protein sequences. GPR35a, which encodes a 309 amino acid, 7-transmembrane domain polypeptide, and GPR35b, which is identical in sequence apart from containing a 31 amino acid N-terminal extension (Okumura et al., 2004). Although the majority of literature on human GPR35 focusses on the short (GPR35a) isoform, it is important to note that there is limited information currently available on whether GPR35a and GPR35b are differentially regulated and/or provide different functionalities in vivo. In human gastric cancer, there does appear to be some differences between the two transcripts with GPR35b being identified from tumors and non-tumorous surrounding regions whilst GPR35a was found in the tumorous regions only, at a level lower than GPR35b, but with a higher transforming capability (Okumura et al., 2004). Such differences were not observed in primary cardiomyocytes where GPR35a and GPR35b mRNA transcripts were found to be expressed to similar levels and to respond in a similar manner to stimuli (Ronkainen et al., 2014). Moreover, in vitro pharmacological efforts using both the long and short isoforms of GPR35 indicated that they respond with similar potency to GPR35 agonists (Guo et al., 2008; MacKenzie et al., 2014). As such, any distinctiveness in function between the splice variants is not likely to reflect

pharmacological variation but it is possible that the extended N-terminal domain of GPR35b will provide protein-protein interactions in a native setting that would not be evident in transfected cell systems (Mackenzie and Milligan, 2015). This, however, has yet to be explored directly. Production of these two transcript variants has only been reported for human, with transcripts akin only to the short version of human GPR35 identified in mouse and rat. Mouse GPR35, which shares 73.4% overall protein sequence identity with human GPR35a, translates into a protein of 307 amino acids from chromosomal locus 1D, whilst rat GPR35, which shares 72% overall homology with human and 85% overall homology with mouse, encodes a protein of 306 amino acids from a chromosome location of 9q36 (Taniguchi et al., 2006).

In an early study investigating coupling of human GPR35a and GPR35b to native neuronal signaling pathways and effectors, human GPR35 isoforms were transiently transfected into cultured rat superior cervical ganglion neurons and the effect on whole cell calcium channel currents (ICa) monitored using the patch-camp technique (Guo et al., 2008). Using a double pulse voltage protocol it was observed that the major component of current originated from N-type calcium channels (Cav2.2). The N-type calcium channel is widely expressed in the CNS and controls neurotransmitter release, together with P/Q- and R-type channels (Mackenzie and Milligan, 2015). These channels are localized to presynaptic terminals, where their voltage-dependent activation leads to an influx of calcium ions, which in turn initiates exocytosis of synaptic vesicles containing various neurotransmitters (Wheeler et al., 1994). Under native conditions, there was no reduction in ICa following application of kynurenic acid (300 μM) or zaprinast (10 μM) to cultured rat superior cervical ganglion neurons. However, when human GPR35 was transiently expressed in these cells, kynurenic acid and zaprinast inhibited ICa currents by 38% and 59%, respectively (Guo et al., 2008). This led the authors to suggest that endogenous expression of rat GPR35 was absent from superior cervical ganglion neurons. However, gene expression or immunocytochemistry were lacking in this report. Despite this, an interesting finding from this paper was the observation that GPR35 appeared to modulate ICa through Gβγ subunit activity, as voltage-dependent inhibition presented with slowed prepulse activation and partially relieved the inhibition of the depolarizing conditioning pulse following application of GPR35 agonists (Guo et al., 2008). This profile was abolished

following application of pertussis toxin, suggesting the involvement of a GPR35-Gi/o coupled pathway. Fast synaptic transmission is mediated synergistically by multiple types of high-voltage-activated Ca channels, including N-type calcium channels, in the mammalian CNS. Therefore, it is interesting that application of GPR35 agonists to rat hippocampal slices endogenously expressing GPR35 generated a concentration and time-dependent reduction in the frequency of spontaneous action potentials in (CA)1 stratum radiatum interneurons (Alkondon et al., 2015). Responses to zaprinast, dicumarol, amlexanox, and pamoic acid were monitored using a standard patch-clamping technique and acted to reduce the frequency of fast current transients (Alkondon et al., 2015). The GPR35 antagonist/inverse agonist ML-145 (1 mM), meanwhile, displayed the reverse effect and significantly increased the mean frequency of fast current transients. Moreover, co-application of ML-145 (1 mM) with zaprinast (10 mM) significantly reduced the inhibitory effect of zaprinast (Alkondon et al., 2015). Despite the issues with the reported lack of affinity of ML-145 at rat GPR35 (Jenkins et al., 2012), in these studies the rank-order of potency of a range of agonists was similar to that observed when employing in vitro pharmacological methods using fluorescently-tagged and overexpressing cell systems to define ligand structure-activity relationships at GPR35 (Divorty et al., 2015). Agonism of GPR35 has also been demonstrated to be involved in the reduction of evoked excitatory post synaptic currents at the CA1 pyramidal neurons of the rat hippocampus, through application of both zaprinast and kynurenic acid (Berlinguer-Palmini et al., 2013). To attempt to eliminate effects independent of GPR35 (e.g. being through kynurenic acid inhibition of NMDA and a-7 nicotinic receptors, or zaprinast inhibition of PDE5 and/or PKG), specific inhibitors were employed, and these did not affect the evoked excitatory postsynaptic current in the same manner as kynurenic acid and zaprinast. Furthermore, the effect of these ligands was ablated following pre-incubation with the GPR35 antagonist/inverse agonist, CID-2745687 (Berlinguer-Palmini et al., 2013). Although the same issues of reported species specificity of CID- 2745687 (Jenkins et al., 2012) clouds interpretation, in conjunction with the previously described findings it seems possible that GPR35 agonists may act to reduce the frequency of action potentials through inhibition of N-type calcium channels, leading to a smaller Ca

influx, a reduction in neurotransmitter release and a reduction in the evoked post synaptic current (Mackenzie and Milligan, 2015).

Recent it was observed that a substantial number of compounds with mast cell stabilizing activity are also agonists of GPR35; these include luteolin, quercetin, ellagic acid, gallic acid, dicumarol, furosemide, nedrocromil, nivimedone, cromolyn, lodoxamide, bufrolin, amlexanox, pemirolast and doxantrazole (Jenkins et al., 2010; Yang et al., 2010; Mackenzie et al., 2014). Moreover, cromolyn was shown to be effective in the treatment of cholangiopathy associated with primary sclerosing cholangitis as a result of reducing mast cell numbers and histamine release (Kennedy, 2007) whilst nedrocromil reduced inflammation and fibrosis in a rat model of colitis (Xu et al., 2002). Although a functional link between GPR35 agonism and mast cell stabilization remains to be demonstrated, GPR35 is expressed in mast cells and is upregulated in response to IgE stimulation (Yang et al., 2010). GPR35 is also highly expressed in basophils and eosinophils (Yang et al., 2010), natural killer cells (Fallarini et al., 2010), CD14 monocytes, dendric cells, peripheral blood lymphocytes, and neutrophils (Wang et al., 2006), suggesting an involvement for this receptor in the immune system and potentially at the neuro-inflammatory axis (Mackenzie and Milligan, 2015).

4.2 Pharmacology

GPR35 retains “orphan” GPCR status despite being able to be stimulated by high concentrations of a number of endogenously produced small molecules, including kynurenic acid, 2-oleoyl lysophosphatidic acid, DHICA (5,6-dihydroxyindole-2-carboxylic acid), reverse T3 (3,3,5-triiodothyronine), cGMP (cyclic guanosine 3050 monophosphate), (Deng and Fang, 2012; Southern et al., 2013), and, most recently, more modest levels of the chemokine CXCL17 (Maravillas-Montero et al., 2015). This reflects that reported estimates of ligand concentration in man, under normal physiological conditions at least, are less than those required to modulate the activity of the receptor substantially (Divorty et al., 2015), or have been described in single publications that have not yet been verified by independent sources (e.g. CXCL17 and derivatives of lysophosphatidic acid). The linkage of endogenously produced molecules with GPR35 activation is further complicated by marked differences in

concentrations required to activate species homologues of this receptor (Milligan, 2011). A further point to note is that additional studies are required to verify the finding that CXCL17 is an/the endogenous ligand of GPR35 before the suggested systematic nomenclature of "CXCR8" (Maravillas-Montero et al., 2015) is agreed upon. Since there is no consensus on the endogenous ligand(s) of this receptor, a large and concerted effort in both academic (Jenkins et al., 2010; Zhao et al., 2010;(Thimm et al., 2013) and industrial (Taniguchi et al., 2006, 2008; Yang et al., 2010, 2012; Deng et al., 2011) sectors; in addition to working collaborations between the two has resulted in reports of a wide range of novel and previously reported small molecule agonists from both distinct, and overlapping, chemical series that are able to activate GPR35. Such ligands include zaprinast, pamoic acid, YE- 120, YE-210, tyrphostin-51, compound 1/TC-G 1001, PSB-13253, lodoxamide, bufrolin, amlexanox, furosemide and cromolyn (Taniguchi et al., 2006; Zhao et al., 2010; Deng et al., 2011; Mackenzie et al., 2014; Jenkins et al., 2010; Yang et al., 2010,). Because screening for GPR35 active ligands has predominantly used the human orthologue, all of these compounds have some level of potency at human GPR35 (Mackenzie and Milligan, 2015). Various agonist ligands display marked differences in efficacy in distinct screening assays, and the implications of this for biological activity in cells and tissues that express GPR35 endogenously remain unclear. Moreover, as the vast majority of ligands with GPR35 agonist activity have derived from screening of commercially available compound libraries, many of the ligands identified from these screens are known to have significant and prominent effects at biological targets other than GPR35. It is vital, therefore, that potential non-GPR35-mediated effects of such ligands are considered (Mackenzie and Milligan, 2015).

Although substantial progress has been made in identification of agonists of GPR35, the identification and/or reporting of GPR35 antagonists has lagged behind. Indeed, representatives from only two chemical series are widely available. Key exemplars of these series are CID-2745687 (1-(2,4-difluorophenyl)-5-[[2-[[(1,1-dimethylehyl)amino]thioxomethyl]hydrazinylidene]methyl]-1Hpyrazole-4- arboxylic acid methyl ester) and ML-145 (2-hydroxy-4-[4-(5Z)-5-[(E)-2-methyl-3-phenylprop-2-enylidene]-4-oxo-2-sulfanylidene-1,3-thiazolidin-3yl]butanoylamino]benzoic acid) (Zhao et al., 2010). Although far from fully characterized, there are no reports of

substantial offtarget effects of these compounds when used at modest concentrations. Indeed, in both these examples there is marked selectivity between GPR35 and GPR55, the most closely related member of the GPCR family. These ligands should, be expected to offer an opportunity to define contributions of GPR35 (Mackenzie and Milligan, 2015). However, the use of these compounds is complicated substantially by their marked species selective behavior. Although not evident initially (Zhao et al., 2010), in transfected cell expression systems both CID- 2745687 and ML-145, although derived from entirely distinct chemical series, were both found to display high affinity at human GPR35 but to display no significant affinity for either the rat or mouse orthologues. This was the case whether monitoring their capacity to block agonist function at GPR35 in transfected cell systems using either b-arrestin-2 recruitment, receptor internalization, or G protein-mediated signaling pathways (Jenkins et al., 2012). Despite the apparent clarity of the in vitro pharmacological studies (Jenkins et al., 2012), initial experiments did report GPR35 antagonism with CID-2745687 at the mouse orthologue in a transfected cell system (Zhao et al., 2010) and, subsequently, a number of functional studies have employed these antagonists in rodent models to prevent apparent GPR35 agonist responses (Berlinguer-Palmini et al., 2013; Alkondon et al., 2015). Clearly further studies perhaps performed in knockout animals (Min et al., 2010) are required to clarify these discrepancies.

4.3 GPR35 and pain

GPR35 has been shown to be highly expressed in the DRG of both rats and mice (Ohshiro et al., 2008; Cosi et al., 2011). GPR35 has been observed in a subpopulation of small diameter sensory neurons expressing TRPV1 (transient receptor potential cation channel subfamily V member 1), a marker of nociceptors. GPR35 expression was observed also in larger sized neurons that convey non-nociceptive information (such as touch and light pressure), which not expressed TRPV1 (Ohshiro et al., 2008). Functional studies demonstrating activation of GPR35 and a reduction in pain perception have employed the acetic acid writhing test (Cosi et al., 2011). Mice were pre-treated by subcutaneous injection with suitable doses of either zaprinast or L-kynurenin, a kynurenic acid precursor, and subsequently acetic acid (0.6%) was applied through intraperitoneal injection. Writhing behavior was then monitored. 5

mg/kg zaprinast and 100 mg/kg L-kynurenine significantly reduced writhing behavior by 54% and 58% relative to phosphate buffered saline-injected control mice (Cosi et al., 2011). Following confirmation of GPR35 expression in the DRG and spinal cord of mice, functional analysis using zaprinast and kynurenic acid on isolated, cultured, glial cells revealed a Gi/o-coupled reduction of cAMP levels following pre-stimulation with forskolin (Cosi et al., 2011). In vivo studies employing the formalin test in rats to investigate the role of zaprinast in visceral pain modulation demonstrated that pre-treatment with zaprinast (10, 30 or 100 mg) by intrathecal injection, followed by subcutaneous injection of formalin (5%) into the planar surface of the hind paw significantly reduced the sum of flinches compared with wild type mice (Yoon et al., 2005). Specifically, zaprinast reduced flinching behavior during phase one and two of the formalin test. The acute phase of the formalin test predominately represents C-fiber activation as a result of peripheral stimulation (Martindale et al., 2001; McCall et al., 1996), whereas the tonic phase typically represents the inflammatory response emanating from the initial stimulus, suggested to be a result of NMDA receptor activation (Vaccarino et al., 1993). The PDE5 inhibitor sildenafil and nonsteroidal anti-inflammatory drugs reduce writhing behavior only at the late phase of the formalin test (Mixcoatl-Zecuatl et al., 2000), while systemic morphine reduces both phases (Capuano et al., 2009). Interestingly morphine acts in a synergistic manner with zaprinast, indicating that zaprinast and morphine act through distinct processes to modulate nociceptive behavior (Mackenzie and Milligan, 2015).

II. Aim of the project

5. Aim of the project

Chemotherapy-induced peripheral neuropathy (CIPN) is the most common neurologic complication of cancer treatment, particularly with the use of platinum-derived agents. Unfortunately, no neuroprotective strategy is yet available for prevention and treatment of CIPN. In the past few years, a prominent role for HCN channels has emerged in both inflammatory and neuropathic pain. Indeed, several studies have reported (1) enhanced HCN channels expression and Ih density in peripheral pain pathway following neuronal damage or inflammation and (2) an analgesic effect of HCN blockers such as ZD7288. However, the role of HCN channels in CIPN is still unclear.

The main goal of the first part of this project was to elucidate the role of HCN channels in CIPN. To this aim, we investigated the possible changes in the physiology of HCN channels in DRG neurons from oxaliplatin treated rats, and evaluated the potential analgesic effects of the HCN blocker ivabradine.

Since non-selective HCN channels blockers could have severe cardiovascular and neurological complications, in the second part of this project we tested the possibility to indirectly modulate HCN channels in order to exert a similar antinociceptive effect. Indeed, it is well established that HCN2 and 4 are cAMP sensitive. Moreover, prostaglandin E2 (PGE2) an important inflammatory mediator activates Adenylate Cyclase (AC) thus increasing intracellular cAMP levels, leading to HCN2 hyper-activation. Based on this molecular mechanism, we hypothesise that Gi coupled receptors activation could counteract PGE2-induced modulation of HCN2 channels, reducing the small DRG neurons excitability and pain transmission. Due to the problems associated with important analgesic drugs such as opioids, we focused on G-protein coupled receptor 35 (GPR35), a completely different target. We previously demonstrated that GPR35 is expressed in DRG neurons and that its activation by

kynurenic acid or zaprinast exert analgesic effect in an *in vivo* model of inflammatory pain (Cosi et al., 2011).

Our data suggest that in oxaliplatin model of CIPN, HCN channels have a prominent role in maintaining neuropathy, and regulating nociceptor excitability. Finally, we demonstrated that it is possible to modulate HCN channels at peripheral level by GPR35 activation.

III. Methods

6. Methods

6.1 Animals

All animal manipulations were carried out according to the European Community guidelines for animal care (DL 116/92, application of the European Communities Council Directive 86/609/EEC) and the local bioethics committee approved all experiments. Housing, handling and killing were in compliance with the Council Directive 2010/63EU and the Council of 22 September 2010. The experimental protocols were approved by the Animal Care Committee of the Department of Neurofarba, University of Florence.

6.2 Oxaliplatin model of CIPN

Rats treated with oxaliplatin (2.4 mg kg-1) were administered intraperitoneally (i.p.) for 5 consecutive days every week for 2 weeks (10 i.p. injections). Oxaliplatin was dissolved in 5% glucose solution. Control animals received an equivalent volume of 5% glucose i.p. (vehicle).

Behavioral tests, for altered pain sensitivity, were performed when neuropathy was established.

Ivabradine treatment: ivabradine was dissolved in saline solution. Acute measures were performed after the intraperitoneal administrations of the drug. Behavioral tests were carried out after 30, 60, 120 and 180 minutes. Control animals were treated with vehicle.

6.3 DRG neurons culture

Rat dorsal root ganglion (DRG) neurons were isolated from both adult (250 – 300 gr) and neonatal (P7-P10) Wistar rats, killed by cervical dislocation followed by decapitation. DRG neurons were prepared as previously described (Vellani et al.,

2004). Briefly, 20–30 ganglia were isolated, incubated in collagenase (2.5 mg ml−1) for 1 h at 37° C and mechanically triturated with sterile needle. The cell suspension was filtered in 40 μm Nylon filter (BD Falcon) then centrifuged and re-suspended in Dulbecco's modified Eagle's medium (DMEM, Gibco) supplemented with 50 u ml−1 penicillin and 0.05 mg ml^{-1} streptomycin (Invitrogen), 1% L-glutamine (Invitrogen), 10 % fetal bovine serum (FBS, Gibco), 50 ng ml−1 nerve growth factor (NGF, Promega) and 1.25 μg ml−1 cytosine β-D-arabinofuranoside (Ara-C, Sigma). DRG neurons were plated onto 13 mm borosilicate cover glass previously coated with polyL-lysine (100 μg ml−1, Sigma) and laminin (10 μg ml-1, Sigma). The medium was changed after 24h. All electrophysiology recordings were made within 72 h from dissociation. DRG neurons were classified based on diameter of somata as follows: small (<26 μm), medium (26 – 35 μm) and large (> 35 μm).

6.4 Immunocytochemistry

24h after the isolation DRG neurons were fixed in 4% formaldehyde and incubated in phosphate buffered saline (PBS) containing 0.1% Triton X-100, 1% BSA, and rabbit anti-GPR35 antibody (1:200 dilution; Abcam) and rabbit anti-HCN2 antibody (1:500; Abcam) for 2h at RT. After washing neurons were incubated with secondary antibodies conjugated to AlexaFluor-488 or Cy3 (1:1000; Invitrogen) for 1h at RT. Relative fluorescence was quantified using ImageJ software (NIH, Bethesda, USA).

6.5 Electrophysiology

Whole-cell recordings: Voltage clamp experiments were performed using a PC-505B amplifier (Warner, Handen, CT, USA) and digitaized with a Digidata 1440 A and Clampex 10 (Axon, Sunnyvale, CA, USA). Pipettes, resistance 3-4.5 MOhm, were pulled from borosilicate capillaries (Harvard Apparatus, London, UK) using a Narishige PP830 vertical puller (Narishige International Ltd, London, UK). Access resistance was monitored during whole-cell voltage clamp recordings throughout experiments with short, -10 mV steps. Recordings undergoing ≥ 10% drift in access resistance were discarded. Pipette capacitance transients were cancelled while no whole-cell compensation was used. Signals were sampled at 10 kHz and low-pass

filtered at 1 kHz. All recordings were made at 21-22°C. Ih was activated with a two-step protocol, consisting of a sequence of hyperpolarizing voltage steps (1.5 s) from -50 to -140 mV, followed by a step at -140 mv (holding potential -60 mV). Ih activation curves were obtained plotting the Ih tail currents against each imposed potential and fitted with a Boltzmann equation of the following form:

$$It / It(max) = 1 / (1 + \exp[(Vm - V½) / k]$$

Where Vm is the membrane potential, V½ is the membrane potential at which Ih is half-activated, k is the slope factor, It is the current amplitude of the tail current recorded for a given pre-pulse and It (max) is the maximum current amplitude of the tail current.

Neuronal excitability was studied applying increasing steps of depolarizing current (500 ms, 50 pA), until generation of the first Action Potential (AP). To study AP threshold dVm/dt was plotted against voltage. AP threshold was estimated as previously reported (Sekerli et al., 2004).

Solutions: Extracellular solution contained (in mM): 140 NaCl, 2 CaCl2, 1 MgCl2, 3 KCl, 10 Hepes, 10 D(+) glucose, adjusted to pH 7.3 with NaOH, osmolarity 300-310 mosmol l-1. Pipette were filled with an intracellular solution containing (in mM): 140 K+-gluconate, 10 HEPES, 5 EGTA, 2 MgCl2, 5 Na2Pcreatine, 0.3 NaGTP, 2 MgATP and adjusted to pH 7.3 with KOH, osmolarity 310-315 mosmol l-1. Cells were continuously perfused with extracellular solution using gravity-fed perfusion system. All substances used were stocked 1000 fold concentrated to avoid freeze/thaw circles. All substances was dissolved in dimethyl sulfoxide (DMSO) unless otherwise specified. Final concentration was respectively: forskolin (Sigma) 50 µM, PGE2 (Sigma) 20 µM, Zaprinast (Tocris) 1 µM, KYNA (Tocris) 30 µM, D-APV (Tocris) 50 µM solved in water, Methyllycaconitine citrate (MLA) (Tocris) 100 nM dissolved in water and ZD7288 (Tocris) 50 µM dissolved in water.

In GPR35 experiments, cultured DRG were incubated with vehicle, KYNA or zaprinast for 20’ at 37 C° in culture medium, than they were moved to the patch clamp setup for electrophysiology recordings. Experiments with KYNA were performed in presence of the NMDA antagonist D-APV (50 µM) and the α7 nicotinic receptor antagonist MLA (100 nM). Experiments with zaprinast were performed in presence of

the phosphodiesterase inhibitor 3,7-Dihydro-1-methyl-3-(2-methylpropyl)-1H-purine-2,6-dione (IBMX) (1 mM).

6.6 Behavioral test

Paw Pressure test: The nociceptive threshold in the rat was determined with an analgesimeter (Ugo Basile, Varese, Italy), as previously described (Leighton et al., 1988). Briefly, a constantly increasing pressure was applied to a small area of the dorsal surface of the paw using a blunt conical probe by a mechanical device. Mechanical pressure was increased until vocalization or a withdrawal reflex occurred while rats were lightly restrained. Vocalization or withdrawal reflex thresholds were expressed in grams. Rats scoring below 40 g or over 75 g during the test before drug administration were rejected. For analgesia measures, mechanical pressure application was stopped at 150 g. All experiments were performed by a researcher blind to drug treatment.

Plantar test: The Hargreaves radiant heat method was carried out as demonstrated by (Tao et al., 2004). The rats were placed individually in clear plastic chambers of Ugo Basile plantar test apparatus for 20 minutes prior to the experiment for the purpose of adaptation. Heat stimulation was applied at IR 60 (infrared intensity 50) on the paw with a 30-second cut-off time. The paw withdrawal latency comprised the time from the start of the beam light until the animal withdrew the paw from the heat stimulus (reaction time) was measured.

Von Frey test: The animals were placed in equipped with a metallic meshy floor, 20 cm above the bench. A habituation of 15 min was allowed before the test. An electronic Von Frey hair unit (Ugo Basile, Varese, Italy) was used: the withdrawal threshold was evaluated by applying force ranging from 0 to 50 g with a 0.2 g accuracy. Punctuate stimulus was delivered to the mid-plantar area of each anterior paw from below the meshy floor through a plastic tip and the withdrawal threshold was automatically displayed on the screen. Paw sensitivity thresh- old was defined as the minimum pressure required to elicit a robust and immediate withdrawal reflex of the paw. Voluntary movements associated with locomotion were not taken as a withdrawal response. Stimuli were applied on each anterior paw with an interval of 5 s. The measure was repeated 5 times and the final value was obtained by averaging the 5

measures (Sakurai et al., 2009).Hot plate. Wistar rats were injected intraplantar (i.pl.) with 50 µl of PGE2 (0.75 nmol), or vehicle, into the left hind paw. A third group of animals were treated intraperitoneal (i.p.) with vehicle or Zaprinast (1; 5; 10 mg/Kg) or KYNA (100; 200; 300 mg/Kg) 20 min before receiving PGE2. 20 min after PGE2 injection, animals were placed on the hot plate device set to 47.5 °C. The latency of licking or flinching response of the left paw was measured in all groups. The cut-off time was set to 60 s to minimize skin damage.

6.7 Data analysis and Statistics

All datasets were tested for approximation to a normal distribution using Graphpad Prism software (D'Agostino test). Datasets were then analyzed using parametric statistical tests (t test for single comparisons or one-way analysis of variance [ANOVA] with Bonferroni post-hoc correction for multiple comparisons). Mean differences were considered significant for $p < 0.05$ *; $p < 0.01$ **; $p < 0.001$ ***.

IV. Results

7. Results I

7.1 Ih current density is enhanced in primary sensory neurons cultured from oxaliplatin-treated rats

In the first series of experiments, we used whole-cell patch clamp technique and the standard two-step voltage clamp protocol (DiFrancesco et al., 1986) to characterize Ih currents in primary sensory neurons from both control (CTRL) and oxaliplatin treated group (OXA). We found that oxaliplatin treatment enhanced the Ih current density in small and medium size neurons. Ih current density was measured at the test step of -100 mV. In small DRG neurons from control group Ih density was -1.43 ± 0.29 pA/pF (n = 15) while in the same class of neurons from oxaliplatin treated rats Ih density was strongly enhanced -3.27 ± 0.62 (n = 13; p = 0.009 CTRL vs OXA). Interestingly differences in Ih current density between small DRG neurons of the two group remain significantly at near resting potentials (-80 mV; p = 0.016 CTRL vs OXA). In medium size neurons we found the same results (Ih density: CTRL -1.65 ± 0.43 pA/pF; n = 6. OXA -5.69 ± 1.61 pA/pF n = 7. P = 0.046 CTRL vs OXA). Interestingly no significant differences in non-nociceptive large size neurons are observed among the DRG cultured from the two group of animal (Ih density: CTRL -2.87 ± 1.56; n = 5. OXA

-5.48 ± 1.19; n = 6. p = 0.210 CTRL vs OXA) indicating an alteration in the expression or function of HCN channels.

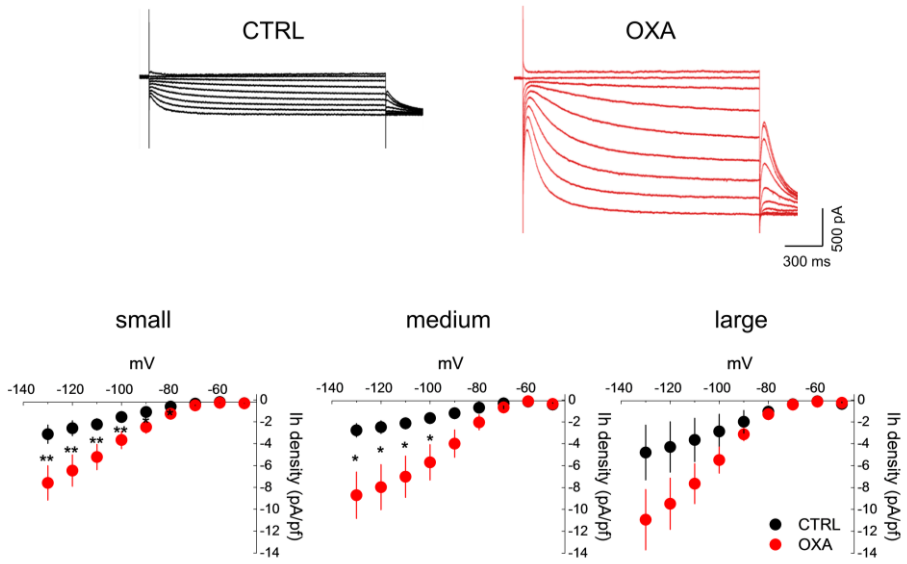

Figure 3 Ih current density is enhanced in primary sensory neurons cultured from oxaliplatin-treated rats.A Whole-cell patch clamp recordings obtained with the standard two-step voltage clamp protocol (DiFrancesco et al., 1986) in order to characterize Ih currents in primary sensory neurons from both control (CTRL) and oxaliplatin treated animals (OXA). B Ih current density in small, medium and large size DRG neurons were measured.. Interestingly, in small and medium DRG neurons Ih density from oxaliplatin treated rats was increased (Ih current density was measured at the test step of -100 mV; CTRL -1.43 ± 0.29 pA/pF, n= 15 versus -3.27 ± 0.62 , n=13; p=0.0099 in small DRG neurons, CTRL vs OXA, respectively, and ctrl -1.65 ± 0.43 pA/pF; n=6 versus -5.69 ± 1.61 pA/pF, n = 7; p = 0.0467 in medium DRG neurons, CTRL vs OXA, respectively). Interestingly, no significant differences in non-nociceptive large size neurons were observed among the DRG cultured from the two group of animal (Ih density: CTRL -2.87 ± 1.56 pA/pF; n = 5. OXA -5.48 ± 1.19 pA/pF; n = 6. P=0.2104 CTRL vs OXA) thus suggesting a selective modification of Ih amplitude and density solely in DRG nociceptors.

7.2 HCN channels open probability is increased in primary sensory neurons cultured from oxaliplatin-treated rats

We further studied the voltage dependence of the HCN channels activation and we observed that oxaliplatin treatment induced a shift of the voltage dependence of these channels towards more depolarized potentials. The activation curve of the HCN channels was obtained plotting the amplitude of the tail current obtained at the full activating step of -140, against each imposed potential. In small DRG neurons the half activation value of the curve (V½) in CTRL was -100.02 ± 1.69 mV (n = 10), while in OXA was more depolarized -95.22 ± 0.80 mV (n = 9; p = 0.024). In medium DRG

neurons the difference is more evident (CTRL -91.36 ± 0.89 mV; n = 7. OXA -86.60 ± 0.51 mV; n = 7. p = 0.0006) while in large non-nociceptive neurons we observed the opposite effect, the Ih activation curve was shifted to more hyperpolarized potential (-86.98 ± 1.60 mV; n = 5. OXA -92.10 ± 0.50 mV; n = 6. p = 0.0091). These results indicated a significant increase of the open probability of the HCN channels at physiological potential in nociceptive neurons.

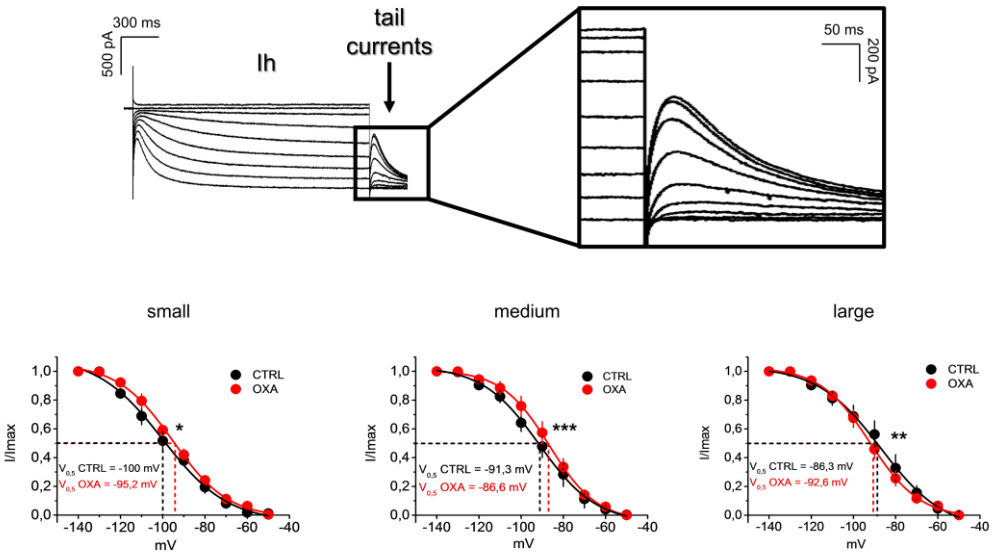

Figure 4 Top: example trace of Ih current of medium DRG neuron. Tail current (square) are obtained with a final step at -140 mV for each imposed potential. Bottom: HCN channels open probability is increased in primary sensory neurons cultured from oxaliplatin-treated rats as indicate by a shift of the Ih activation curve towards more depolarized potentials.

7.3 Administration of ivabradine exerts analgesic effect in an model of CIPN

To study the role of HCN channels in an in vivo model of Chemotherapy-Induced Peripheral Neuropathy (CIPN) we used the HCN channels blocker ivabradine (IVA). Animals were treated with ivabradine 5 mg/Kg at day 15 of oxaliplatin treatment, and the behavioral tests were performed for 3h right after ivabradine injection. We performed the paw pressure test to evaluate the mechanical hyperalgesia, the Von Frey test to asses the mechanical allodynia and the plantar test to evaluate the thermal

hyperalgesia. We found that subcutaneous injection of ivabradine in neuropathic animals induced a strong and transient analgesic effect on both mechanical and thermal stimuli. At 0 time point neuropathic animal showed a paw pressure threshold of 42.92 ± 1.04 g (n = 6) while in control animal was 64.43 ± 1.55 g (n = 6 p = 5.0E-10). After 60' from ivabradine injection the paw pressure threshold were nearly restored to control value (OXA + veh 43.95 ± 0.62 g; n = 6. OXA + IVA 59.43 ± 0,56 g; n = 6. p = 8.8E-9). Also the Von Frey threshold was significantly enhanced 1 hour after the injection (OXA + veh 22.11 ± 1,48 g; n = 6. OXA + IVA 11.85 ± 0.64; n = 6. p = 4.45E-8). The same results were obtained for thermal hyperalgesia measured with the

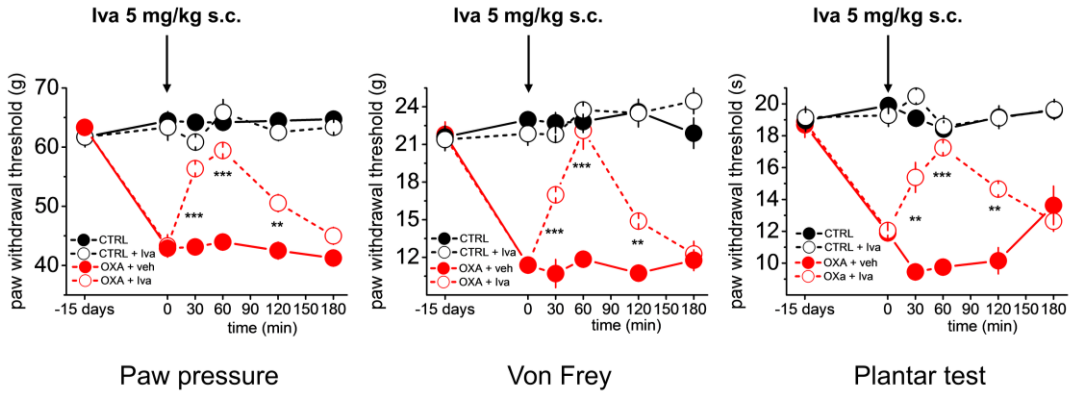

Figure 5 Administration of ivabradine exerts analgesic effect in an in vivo model of CIPN. Ivabradine exert a strong and transient analgesic effect peacking at 60' after the injection. Interestingly no effects were observed injecting ivabradine in control animals, indicating that ivabradine does not affect the physiological transmission of thermal and mechanical stimuli.

plantar tests 60' after the ivabradine injection (OXA + veh 9.75 ± 0.35 s; n = 6. OXA + IVA 17.25 ± 0.30 s; n = 6. p = 7.45E-8). All threshold values gradually returned to the levels prior to ivabradine injection. Interestingly no effects were observed injecting ivabradine in control animals for all three test performed. (Plantar test at 60': CTRL 17.23 ± 0.4 s, n = 6; CTRL + IVA 17.31 ± 0.6 s, n = 6. Von Frey test at 60': CTRL 22.12 ± 0.87 g, n = 6; CTRL + IVA 23.05 ± 0.33 g, n = 6. Paw pressure test at 60': CTRL 64.16 ± 0.83 g, n = 6; CTRL + IVA 65.83 ± 2.20 g, n = 6.). These results suggest

an important contribution of HCN channels in maintaining peripheral neuropathy without affecting the physiological transmission of mechanical and thermal stimuli.

8. Results II

8.1 GPR35 and HCN2 are co-expressed in small primary sensory neurons from dissociated rat DRG

To study the expression of GPR35 and HCN channels in different population of DRG neurons, we used immunofluorescence. We found that GPR35 and HCN2 immunoreactivity was present in small, medium and large with the highest relative florescence for both GPR35 and HCN2 in the small DRG neurons.

We then used the standard two-step voltage clamp protocol (DiFrancesco et al., 1986) to characterize Ih currents. In agreement with the literature (Kouranova et al., 2008; Mayer and Westbrook, 1983; Scroggs et al., 1994), we found that in our preparation the Ih amplitude was 125 ± 52 pA at the test step of -110 mV (Fig. 6B, red trace) and that the Ih activation curve had a V½ of -100.6 ± 1.9 mV. The HCN blocker ZD7288 (50 μM for 10') fully abolished Ih current (Fig. 6B top-right). Interestingly, pharmacological Ih suppression had no discernible effect on RMP (-54.8 ± 2.0 mV to -55.1 ± 3.2 mV, n = 6, p = 0.7, ctrl vs ZD7288, respectively; Fig. 6B bottom-right)

showing that the control of the RMP in small DRG neurons differs from that of other neuronal cell types (Biel et al., 2009; Masi et al., 2013).

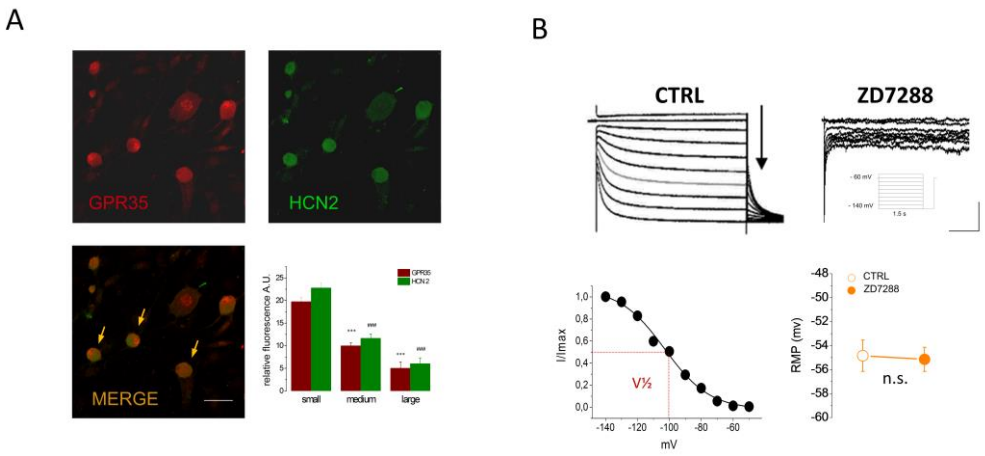

Figure 6 GPR35 and HCN2 are co-expressed in rat DRG small primary sensory neurons. A. Immunofluorescent detection of GPR35 (top left) and HCN2 (top right) in rat DRG neurons. Small double-labeled neurons are indicated by arrows. (Scale bar = 50 µm). Histogram, mean fluorescence intensity of GPR35 and HCN2 signal in small (n = 50), medium (n = 42) and large (n = 35) DRG neurons. ***B****. Characterization of Ih current in small rat DRG neurons. Top, whole cell current traces before (ctrl) and after application of Ih-blocker ZD7288. Black arrow indicates tail currents at the -140 mV step. Inset, protocol scheme, scale: 250 ms, 150 pA. Bottom left, Ih activation curve obtained plotting the tail currents amplitude against each imposed potential. Bottom right, scatter graph representing the resting membrane potential before and after the ZD7288 mediated HCN channels blockade, no changing in RMP are observed.*

8.2 GPR35 agonists counteract forskolin effect on RMP and Ih activation curve

When DRG neurons were exposed to forskolin (FRK, an activator of adenylate cyclase), Ih activation curves were shifted towards more positive potentials leading to RMP depolarization and increasing cell excitability (Momin et al., 2008). As shown in Fig. 7A, FRK application caused a mean RMP depolarization of 5 mV (-56.5 ± 1.1 to -51.6 ± 1.2 mV, n = 8, p = 7.5E-4, ctrl vs FRK, respectively) and induced a ~ +15 mV shift of Ih activation curve (V½ -100.6 ± 1.9 mV to -85.4 ± 1.6 mV, n = 12, ctrl vs FRK, respectively). These effects were completely prevented by pre-incubation with Ih blocker ZD7288 (-57.2 ± 1.9 to -57.3 ± 2.1 mV, n = 6, ZD7288 vs ZD7288 + FRK, respectively).

In order to study the effects of GPR35 activation on forskolin-induced Ih changes we used KYNA and zaprinast. Since the effects observed after KYNA exposure could be mediated by NMDA (Stone et al., 2013) or α7 nicotinic acetylcholine receptor

antagonism (Albuquerque and Schwarcz, 2013), all the experiments were performed in presence of maximally active concentrations of the NMDA receptor antagonist D-APV and of the □7 nicotinic antagonist MLA. To avoid that the effects observed after zaprinast exposure could be mediated by its inhibitory action on phosphodiesterase activity, all the experiments involving zaprinast were performed in presence of high concentrations of the phosphodiesterase inhibitor IBMX.

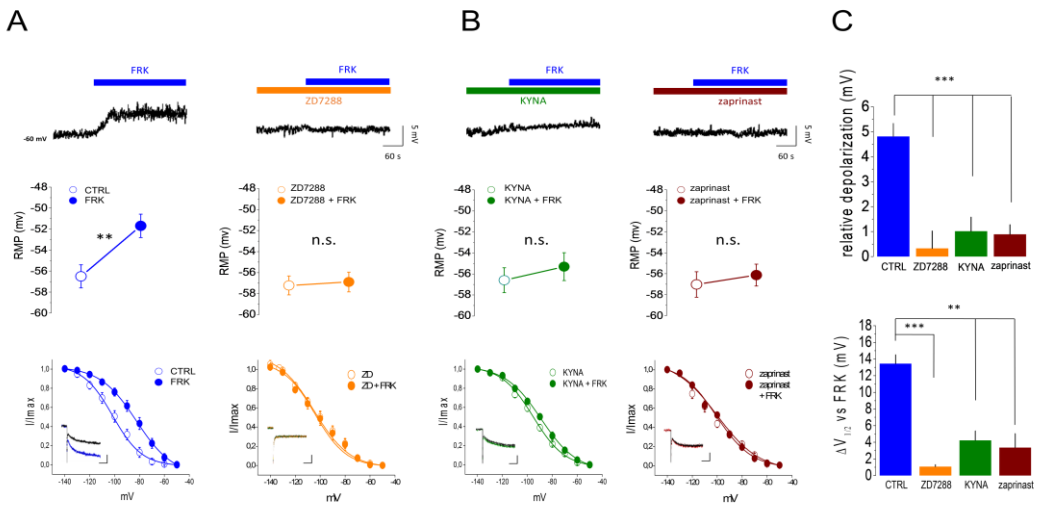

Figure 7 GPR35 agonists counteract forskolin effect on RMP and Ih activation curve A. top, Representative traces of forskolin-induced RMP depolarization, recorded in current–clamp configuration in control condition (left) and in presence of ZD7288 (right). Middle, RMP depolarization quantitative analysis. Bottom, Ih activation curve. In control condition, forskolin shifts the Ih activation curve towards more depolarized potentials, on the contrary in presence of ZD7288 no alteration are observed after forskolin application. Inset, representative traces of Ih current at the voltage step of -90 mV, before and after forskolin application, scale: 250 ms / 50 pA. ***B****. top, Representative traces of forskolin-induced depolarization, in presence of KYNA (left) or zaprinast (right). Middle, RMP depolarization quantitative analysis. Bottom, forskolin effect on the Ih activation curve, in presence of KYNA or zaprinast. In presence of both GPR35 agonists, no alterations of Ih activation curve are observed after application of forskolin. Inset, representative traces of Ih current at the voltage step of -90 mV, before and after forskolin application, scale: 250 ms / 50 pA.* ***C****. top, quantification of the relative depolarization after application of forskolin in control condition, in presence of ZD7288 or in presence of GPR35 agonists. Bottom, ΔV½ of Ih activation curve after forskolin application in all conditions.*

Then we tested the modulation of GPR35 agonists on RMP and Ih activation curve, *per se* and we noticed that neither KYNA nor zaprinast directly affected RMP or Ih activation curve. On the contrary, both KYNA and zaprinast were able to counteract FRK effects (Fig. 7B and 7C). Indeed, both GPR35 agonists significantly reduced FRK-induced depolarization (-56.4 ± 1.2 mV to -54.3 ± 1.5 mV, n = 8, p = 0.14 KYNA vs KYNA + FRK, respectively; -57.0 ± 1.2 mV to -56.1 ± 1.0 mV, n = 8, p = 0.08

zaprinast vs zaprinast + FRK respectively) and FRK-induced rightward-shift of the activation curve (V½ -98.3 ± 0.7 mV to -95.4 ± 0.9 mV, n = 8, KYNA vs KYNA + FRK, respectively; -98.3 ± 0.7 mV to -95.4 ± 0.9 mV, n = 8, zaprinast vs zaprinast + FRK, respectively). Fig. 7C reports the quantitative effects of GPR35 agonists on both RMP (top) and Ih activation curve V½ (bottom).

8.3 GPR35 agonists counteract the effect of PGE2

PGE2 is a powerful endogenous pro-inflammatory mediator and it increases primary sensory neuron excitability by increasing intracellular cAMP levels. It has been demonstrated that application of PGE2 in small DRG neurons leads to an HCN-mediated depolarization (Momin et al., 2008). Therefore, we determined the ability of GPR35 agonists to prevent, or reduce, the electrophysiological effects of PGE2 in small DRG neurons. We observed that PGE2 20 µM induced RMP depolarization

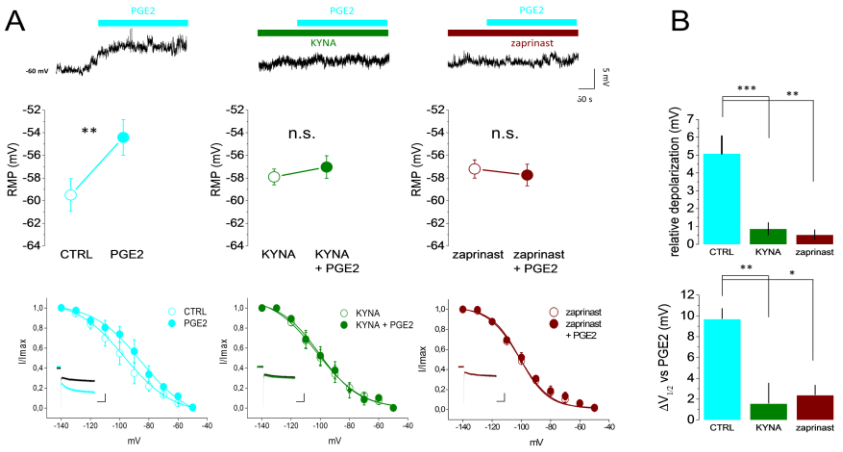

Figure 8 GPR35 agonists counteract the effect of PGE2. A Top, PGE2 50 µM for 4' induced RMP depolarization in control condition (left) in presence of kynA (middle) or zaprinast (right). Bottom, PGE2 induced shift of the Ih activation in control condition in presence of kynA or zaprinast. B. top, quantification of the relative depolarization after application of PGE2 in control condition or in presence of GPR35 agonists. Bottom, ΔV½ of Ih activation curve after PGE2 application in the same conditions.

(from -59.8 ± 1.8 mV to -54.4 ± 1.5 mV, n = 8, p = 0.003) and caused a positive shift of Ih activation curve (V½ from -98.7 ± 0.4 mV to -87.1 ± 0.8 mV, n=8) (Fig. 8A).

Interestingly, both PGE2-induced RMP depolarization and the shift of Ih activation curve were significantly reduced by pre-application of KYNA (RMP from -57.9 ± 0.6 mV to -57 ± 0.9 mV, n = 8, p = 0.08; V½ from 102.3 ± 2.2 mV to -100.5 ± 1.7 mV, n = 8, KYNA vs KYNA + PGE2, respectively) or zaprinast (RMP from -57.2 ± 0.8 mV to -57.7 ± 0.9 mV, n = 8, p = 0.13; V½ from-101.3 ± 1.7 mV to -100.5 ± 1.5 mV, n = 8, zaprinast vs zaprinast + FRK, respectively), thus indicating that GPR35 activation was able to prevent PGE2-dependent RMP depolarization by counteracting the positive shift of Ih activation curve.

8.4 GPR35 agonists counteract the effect of PGE2 on neurons excitability

We then studied the intrinsic excitability of small DRG neurons by performing voltage recordings (see methods). We observed that PGE2 did not affect neither AP firing threshold (-26.9 ± 2.3 mV to 29.8 ± 2.0 mV, n = 8, p = 0.52, ctrl vs PGE2,

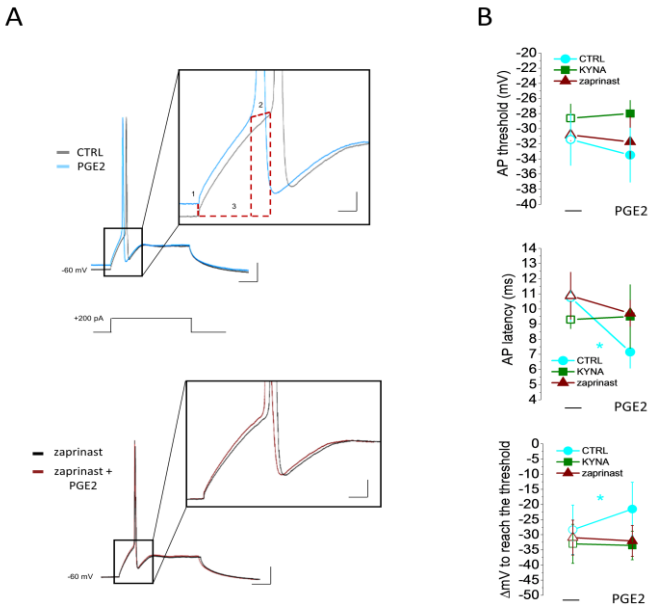

Figure 9 GPR35 agonists counteract the effect of PGE2 on neuronal excitability. Small DRG neuron excitability was studied by applying increasing steps of depolarizing current until generation of a single action potential (AP). ***A****. Example traces of an AP evoked injecting 200 pA of depolarizing current, before and after PGE2 application, scale: 10 ms / 15 mV. In square, magnification of the traces showing the resting potential (1), AP threshold (2) and the latency to reach the threshold (3), scale: 2 ms / 5 mV. Bottom, example traces of the same experiment performed in presence of zaprinast.* ***B****. Scatter graphs showing the PGE2 effect on AP threshold, latency and the ΔmV to reach the threshold, in control condition (circle), in presence of KYNA (square) or zaprinast (triangle).*

respectively); nor AP amplitude or duration (data not shown). Application of PGE2 led to depolarization of the RMP that ultimately reduced AP latency (10.76 ± 1.5 ms to 7.1 ± 1.0 ms, n = 8, p = 0.01, ctrl vs PGE2 respectively) and the depolarization needed to reach AP threshold (ΔmV, -28.3 ± 3.3 mV to -21.5 ± 3.6 mV, n = 8, p = 0.002, ctrl vs PGE2, respectively; Fig. 9B bottom). GPR35 activation prevented small DRG neurons PGE2-induced depolarization therefore no effect on either AP latency (9.3 ± 0.6 ms to 9.5 ± 2.1 ms, n = 8, p = 0.91; KYNA vs KYNA + PGE2, respectively; 10.9 ± 1.3 ms to 10.3 ± 1.4 ms, n = 8, p = 0.51, zaprinast vs zaprinast + PGE2, respectively) or on the depolarization needed to reach AP threshold (-33.0 ± 6.4 mV to -33.5 ± 4.7 mV, n = 8, p = 0.73, KYNA vs KYNA + PGE2, respectively; -30.9 ± 5.7 mV to -32.0 ± 5.0 mV, n = 8, p = 0.083, zaprinast vs zaprinast + PGE2) was observed following PGE2.

8.5 Analgesic effect of GPR35 agonists in a model of PGE2-induced thermal hyperalgesia

Finally, we assessed if GPR35 activation could lead to analgesia in a model of thermal hyperalgesia induced by injecting PGE2 into the hind paw (see methods). Intradermal injection of PGE2 0.75 nmol reduced the paw withdrawal latency in response to heat stimuli (vehicle 58.2 ± 4.9 s n = 13; PGE2 15.6 ± 1.6 s n = 17 p = 7.8 E-17). As shown in Fig. 10A, animals pretreated (20’ before) with KYNA i.p. showed a dose dependent increase in withdrawal latency (PGE2 + KYNA 100 mg/Kg: 22.4 ± 2.6 s, n = 8, p = 1; PGE2 + KYNA 200 mg/Kg: 30.8 ± 5.9 s, n = 9, p = 0.002; PGE2 + KYNA 300 mg/Kg: 44.4 ± 5.7 s, n = 8, p = 1.1 E-7. All p values are vs PGE2). Similarly, zaprinast showed a significant analgesic effect on PGE2-induced hyperalgesia (PGE2 + zaprinast 1 mg/Kg: 19.2 ± 3.3 s, n = 10, p = 0.96; PGE2 +

zaprinast 5 mg/Kg: 32.3 ± 6.1 s, n = 8, p = 0.01; PGE2 + zaprinast 10 mg/Kg: 23.6 ± 4.4 s, n = 9, p = 0.5. All p values are vs PGE2 + veh).

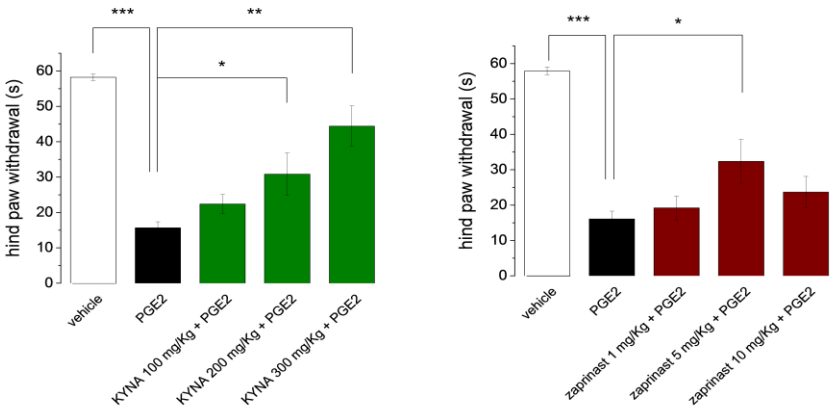

Figure 10 In vivo analgesic effect of GPR35 agonists in a PGE2 model of thermal hyperalgesia. In adult wistar rats hid paw injection of PGE2, generate a hyperalgesic effect in the hot plate test set at 47.5 C°. The latency of the hind paw withdrawal is reduced from 58.2 ± 0.9 s in animals treated with vehicle, to 15.6 ± 1.6 s in animals treated with PGE2. Animals treated with KYNA (left) or zaprinast (right) show a dose dependent analgesic effect.

V. Discussion

9. Discussion

Chemotherapy-induced peripheral neuropathy (CIPN) is the most common neurologic complication of cancer treatment, particularly with the use of platinum-derived agents. Unfortunately, no neuroprotective strategy is yet available for prevention and treatment of CIPN, therefore, testing and validating available protective strategies in preclinical and clinical settings should be the next steps in overcoming platinum-induced peripheral neurotoxicity.

In the past few years, a prominent role for HCN channels has emerged for both inflammatory and neuropathic pain, thus the main goal of the first part of this project was to elucidate the role of the HCN channels in CIPN.

Our first results showed that Ih current density was enhanced in primary sensory neurons cultured from oxaliplatin-treated rats (Figure 3). Moreover, we found a little but significant shift of Ih activation curve towards more depolarized potentials (Figure 4). Finally we demonstrated that ivabradine, a well characterized Ih blocker, exerts analgesic effect for oxaliplatin-induced mechanical hyperalgesia, allodynia and thermal hyperalgesia (Figure 5).

As in other neuropathic pain animal models (reviewed in Herrmann et al., 2015), we found increased Ih density in DRG neurons cultured from oxaliplatin treated rats, indicating an alteration in the expression or function of HCN channels. Moreover, the shift of the voltage dependence of the HCN channels towards more positive potentials indicated an increased open probability of these channels near resting that could lead to depolarization, thus increasing the overall excitability of nociceptive neurons. To better understand the role of Ih current in oxaliplatin-induced neuropathy, we treated neuropathic rats with ivabradine, a clinically used HCN blocker. We observed that ivabradine exert a transient but strong analgesic effect for both mechanical and thermal stimuli, peacking 1h after the injection. Interestingly no effects were observed injecting ivabradine in control animals, suggesting the important role of HCN channels

in maintaining neuropathy without affecting the physiological transmission of mechanical and thermal stimuli.

Taking together these results suggested that HCN channels could participate in developing the hyper-excitability of nociceptive neurons that lead to hyperalgesia and allodynia in vivo. Indeed, the block of these channels leads to a rapid and strong analgesic effect, restoring the physiological transmission of painful stimuli of nociceptive neurons.

However, non-selective HCN channels blockers could have severe complications due to the block of cardiac HCN4 and other off-targets such as potassium (Lees-Miller et al., 2015) and calcium channels (Sánchez-Alonso et al., 2008). Due to these side effects, in the second part of this study we looked for an HCN channels indirect modulation. It is well established that HCN2 and 4 are cAMP sensitive and important inflammatory mediators such as prostaglandin E2 (PGE2) activate the Adenylate Cyclase (AC) thus elevating the cAMP levels, leading to HCN2 hyper-activation (Momin et al., 2008; Emery et al., 2011). Our hypothesis was that the activation of a Gi coupled receptors could reduce the PGE2-induced modulation of HCN2 channels, reducing the small DRG neurons excitability, thus reducing the pain transmission. Due to the problems associated with important Gi-coupled receptors such as opioid receptors, we focused on a completely different target, the G-protein coupled receptor 35 (GPR35). We previously demonstrated that GPR35 is expressed in DRG neurons and that receptor activation with kynurenic acid or zaprinast exert analgesic effect in an *in vivo* model of inflammatory pain (Cosi et al., 2011).

It is possible to increase cellular excitability by exposing cultured nociceptors to either FSK or PGE2 thus increasing the local cAMP availability. Elevated cAMP levels are able to shift the Ih activation curve toward more positive potentials thus leading to cellular depolarization increasing the nociceptors excitability (Emery et al., 2011; Momin et al., 2008). Our results showed that small DRG neurons (nociceptors) expressed significant amount of GPR35 and of HCN2 (Figure 6). Moreover KYNA and zaprinast, two different GPR35 agonists, prevented the FRK and PGE2 mediated effects (Figure 7 and 8), suggesting that the previously observed analgesic actions of these (Cosi et al., 2011) and other GPR35 agents, for instance cromolyn (Leza et al., 1992), may be mediated by changes in HCN2 channel function. Indeed, neither FRK

nor PGE2 were able to modify nociceptors RMP or shift the HCN activation curve when KYNA or zaprinast were present. We also found that the local increase of cAMP induced by either FRK or PGE2 was not associated to changes in AP amplitude, duration or threshold, thus ruling out the involvement of voltage gated Na+ channel in the observed effects. These results are in line with previous observation arguing against a major effect of cAMP increase on voltage-dependent Na+ or K+ currents (Momin et al., 2008). The application of FRK or PGE2 increased neuronal excitability by shifting HCN activation curve and by causing RMP depolarization. Under those conditions, the latency and the further depolarization needed to reach the AP threshold were reduced. In the presence of GPR35 agonists, the HCN-mediated effect of FRK and PGE2 were prevented and the neurons maintained the physiological excitability (Figure 9). In performing the present experiments, we were aware that the two GPR35 agonists that we used are not specific and therefore appropriate controls were carried out. When we used KYNA, we ruled out the possibility that the effects were mediated through the NMDA or α7 nicotinic receptors by adding supra-maximal concentrations of appropriate antagonists (APV and MLA) and all the experiments with zaprinast were performed in the presence of high concentrations of IBMX another phosphodiesterase inhibitor (see methods). We also attempted to antagonize GPR35 activation by using CID 2745687 (1-10 μM) one of the few available receptor antagonist. Unfortunately, the compound had non-expected actions in the system: in particular it reduced Ih amplitude possibly because of a direct interaction with HCN channels. The need of better and less species specific GPR35 agonists and antagonists (Jenkins et al., 2012) could be important in order to better characterize the GPR35 mediated activation of Ih modulation (Mackenzie and Milligan, 2015). In this line, it is interesting to note that we considered KYNA a possible endogenous GPR35 ligand (Wang et al., 2006; Cosi et al., 2011; Moroni et al., 2012). It has been recently reported, however, that the main endogenous GPR35 agonist could be the chemokine CXCL17 (Maravillas-Montero et al., 2015). In spite of this proposal, we observed that low micromolar concentration of KYNA may activate GPR35 in different systems

(Berlinguer-Palmini et al., 2013) and we are still convinced that GPR35 is an interesting target for a new generation of analgesic agents.

In order to further study in vivo the analgesic action of GPR35 agonists we used PGE2 to induce thermal hyperalgesia in rats hind paw. Previous experiments have shown that KYNA precursor L-kynurenine was able to exert antinociceptive effects in the acetic acid model of inflammatory pain by increasing KYNA content in plasma and in the CNS (Cosi et al., 2011). Kynurenine was used because KYNA itself poorly cross the blood brain barrier (Lou et al., 1994). However, since the DRG are located outside the blood–brain barrier (Sapunar et al., 2012) we directly administered KYNA to stimulate GPR35 located in the DRG neurons. We observed a significant analgesic effect even if the doses of KYNA were relatively high (Figure 10). This could be explained by the fact that KYNA is rapidly eliminated in the urine and its plasma concentrations rapidly declines (Chiarugi et al., 1996; Moroni et al., 1988). We also tested zaprinast a more potent GPR35 agonist, which had significance antinociceptive effect at dose of 5 mg/Kg (Figure 10). The bell shaped dose-response curve of zaprinast in vivo is reasonably to be ascribed to phosphodiesterase inhibition with a significant local cAMP accumulation at the highest doses (Taniguchi et al., 2006).

Taking together, GPR35 modulation in immune system, calcium channels and HCN channels in nociceptors, provide the evidence of a promising new target in inflammatory and neuropathic pain.

Our data suggest that in the oxaliplatin model of CIPN, HCN channels have a role in maintaining the neuropathy, regulating the nociceptor excitability. Moreover, we demonstrated for the first time that it is possible to modulate the HCN channels at peripheral level by activating GPR35. GPR35 agonists may act in the DRG neurons and are not required to penetrate the blood brain barrier thus lacking most of the side effects of currently available centrally acting analgesics. Certainly, more studies are needed to find more potent and selective GPR35 agonists.

In conclusion, in this study we demonstrated that HCN channels could be a promising target for management of Chemotherapy-Induced Peripheral Neuropathy and the modulation of these channels could represent a potentials strategy for neuropathic pain treatment.

VII Bibliography

- Acosta, C., McMullan, S., Djouhri, L., Gao, L., Watkins, R., Berry, C., Dempsey, K., Lawson, S. N., 2012. HCN1 and HCN2 in Rat DRG neurons: levels in nociceptors and non-nociceptors, NT3-dependence and influence of CFA-induced skin inflammation on HCN2 and NT3 expression. PLoS One 7, e50442.
- Albers, J. W., Chaudhry, V., Cavaletti, G., Donehower, R. C., 2011. Interventions for preventing neuropathy caused by cisplatin and related compounds. Cochrane Database Syst Rev, CD005228.
- Albers, J. W., Chaudhry, V., Cavaletti, G., Donehower, R. C., 2014. Interventions for preventing neuropathy caused by cisplatin and related compounds. Cochrane Database Syst Rev 3, Cd005228.
- Alberti, P., Rossi, E., Cornblath, D. R., Merkies, I. S., Postma, T. J., Frigeni, B., Bruna, J., Velasco, R., Argyriou, A. A., Kalofonos, H. P., Psimaras, D., Ricard, D., Pace, A., Galie, E., Briani, C., Dalla Torre, C., Faber, C. G., Lalisang, R. I., Boogerd, W., Brandsma, D., Koeppen, S., Hense, J., Storey, D., Kerrigan, S., Schenone, A., Fabbri, S., Valsecchi, M. G., Cavaletti, G., 2014. Physician-assessed and patient-reported outcome measures in chemotherapy-induced sensory peripheral neurotoxicity: two sides of the same coin. Ann Oncol 25, 257-264.
- Ali, I., Wani, W. A., Saleem, K., Haque, A., 2013. Platinum compounds: a hope for future cancer chemotherapy. Anticancer Agents Med Chem 13, 296-306.
- Alkondon, M., Pereira, E. F., Todd, S. W., Randall, W. R., Lane, M. V., Albuquerque, E. X., 2015. Functional G-protein-coupled receptor 35 is expressed by neurons in the CA1 field of the hippocampus. Biochem Pharmacol 93, 506-518.
- Anand, U., Otto, W. R., Anand, P., 2010. Sensitization of capsaicin and icilin responses in oxaliplatin treated adult rat DRG neurons. Mol Pain 6, 82.
- Antal, M., Papp, I., Bahaerguli, N., Veress, G., Vereb, G., 2004. Expression of hyperpolarization-activated and cyclic nucleotide-gated cation channel subunit 2 in axon terminals of peptidergic nociceptive primary sensory neurons in the superficial spinal dorsal horn of rats. Eur J Neurosci 19, 1336-1342.
- Argyriou, A. A., Bruna, J., Marmiroli, P., Cavaletti, G., 2012a. Chemotherapy-induced peripheral neurotoxicity (CIPN): an update. Crit Rev Oncol Hematol 82, 51-77.
- Argyriou, A. A., Cavaletti, G., Antonacopoulou, A., Genazzani, A. A., Briani, C., Bruna, J., Terrazzino, S., Velasco, R., Alberti, P., Campagnolo, M., Lonardi, S., Cortinovis, D., Cazzaniga, M., Santos, C., Psaromyalou, A., Angelopoulou, A., Kalofonos, H. P., 2013. Voltage-gated sodium channel polymorphisms play a pivotal role in the development of oxaliplatin-induced peripheral neurotoxicity: results from a prospective multicenter study. Cancer 119, 3570-3577.

- Argyriou, A. A., Koltzenburg, M., Polychronopoulos, P., Papapetropoulos, S., Kalofonos, H. P., 2008. Peripheral nerve damage associated with administration of taxanes in patients with cancer. Crit Rev Oncol Hematol 66, 218-228.
- Argyriou, A. A., Velasco, R., Briani, C., Cavaletti, G., Bruna, J., Alberti, P., Cacciavillani, M., Lonardi, S., Santos, C., Cortinovis, D., Cazzaniga, M., Kalofonos, H. P., 2012b. Peripheral neurotoxicity of oxaliplatin in combination with 5-fluorouracil (FOLFOX) or capecitabine (XELOX): a prospective evaluation of 150 colorectal cancer patients. Ann Oncol 23, 3116-3122.
- Avan, A., Postma, T. J., Ceresa, C., Cavaletti, G., Giovannetti, E., Peters, G. J., 2015. Platinum-induced neurotoxicity and preventive strategies: past, present, and future. Oncologist 20, 411-432.
- Bao, W., Pan, H., Zhang, Z., Cheng, Y., Xie, Z., Zhang, J., 2015. Isolation of the stable strain Labrys sp. BK-8 for L(+)-tartaric acid production. J Biosci Bioeng 119, 538-542.
- Baruscotti, M., Bucchi, A., Difrancesco, D., 2005. Physiology and pharmacology of the cardiac pacemaker ("funny") current. Pharmacol Ther 107, 59-79.
- Basbaum, A. I., Fields, H. L., 1978. Endogenous pain control mechanisms: review and hypothesis. Ann Neurol 4, 451-462.
- Bender, R. A., Kirschstein, T., Kretz, O., Brewster, A. L., Richichi, C., Rüschenschmidt, C., Shigemoto, R., Beck, H., Frotscher, M., Baram, T. Z., 2007. Localization of HCN1 channels to presynaptic compartments: novel plasticity that may contribute to hippocampal maturation. J Neurosci 27, 4697-4706.
- Bennett, G. J., Xie, Y. K., 1988. A peripheral mononeuropathy in rat that produces disorders of pain sensation like those seen in man. Pain 33, 87-107.
- Berlinguer-Palmini, R., Masi, A., Narducci, R., Cavone, L., Maratea, D., Cozzi, A., Sili, M., Moroni, F., Mannaioni, G., 2013. GPR35 activation reduces Ca2+ transients and contributes to the kynurenic acid-dependent reduction of synaptic activity at CA3-CA1 synapses. PLoS One 8, e82180.
- Bhagra, A., Rao, R. D., 2007. Chemotherapy-induced neuropathy. Curr Oncol Rep 9, 290-299.
- Biel, M., Wahl-Schott, C., Michalakis, S., Zong, X., 2009. Hyperpolarization-activated cation channels: from genes to function. Physiol Rev 89, 847-885.
- Bittar, R. G., Kar-Purkayastha, I., Owen, S. L., Bear, R. E., Green, A., Wang, S., Aziz, T. Z., 2005. Deep brain stimulation for pain relief: a meta-analysis. J Clin Neurosci 12, 515-519.
- Boehmerle, W., Zhang, K., Sivula, M., Heidrich, F. M., Lee, Y., Jordt, S. E., Ehrlich, B. E., 2007. Chronic exposure to paclitaxel diminishes phosphoinositide signaling by calpain-mediated neuronal calcium sensor-1 degradation. Proc Natl Acad Sci U S A 104, 11103-11108.
- Boivie, J., Leijon, G., Johansson, I., 1989. Central post-stroke pain--a study of the mechanisms through analyses of the sensory abnormalities. Pain 37, 173-185.
- Bokhari, F., Sawatzky, J. A., 2009. Chronic neuropathic pain in women after breast cancer treatment. Pain Manag Nurs 10, 197-205.

- Bonica, J. J., 1979. The need of a taxonomy. Pain 6, 247-248.
- Boyette-Davis, J. A., Cata, J. P., Zhang, H., Driver, L. C., Wendelschafer-Crabb, G., Kennedy, W. R., Dougherty, P. M., 2011. Follow-up psychophysical studies in bortezomib-related chemoneuropathy patients. J Pain 12, 1017-1024.
- Briggs, I., BoSmith, R. E., Heapy, C. G., 1994. Effects of Zeneca ZD7288 in comparison with alinidine and UL-FS 49 on guinea pig sinoatrial node and ventricular action potentials. J Cardiovasc Pharmacol 24, 380-387.
- Bucchi, A., Barbuti, A., Baruscotti, M., DiFrancesco, D., 2007. Heart rate reduction via selective 'funny' channel blockers. Curr Opin Pharmacol 7, 208-213.
- Bucchi, A., Baruscotti, M., Nardini, M., Barbuti, A., Micheloni, S., Bolognesi, M., DiFrancesco, D., 2013. Identification of the molecular site of ivabradine binding to HCN4 channels. PLoS One 8, e53132.
- Campbell, J. N., Meyer, R. A., 2006. Mechanisms of neuropathic pain. Neuron 52, 77-92.
- Capuano, A., De Corato, A., Treglia, M., Tringali, G., Dello Russo, C., Navarra, P., 2009. Antinociceptive activity of buprenorphine and lumiracoxib in the rat orofacial formalin test: a combination analysis study. Eur J Pharmacol 605, 57-62.
- Cavaletti, G., 2014. Chemotherapy-induced peripheral neurotoxicity (CIPN): what we need and what we know. J Peripher Nerv Syst 19, 66-76.
- Cavaletti, G., Alberti, P., Marmiroli, P., 2011. Chemotherapy-induced peripheral neurotoxicity in the era of pharmacogenomics. Lancet Oncol 12, 1151-1161.
- Cavanaugh, D. J., Lee, H., Lo, L., Shields, S. D., Zylka, M. J., Basbaum, A. I., Anderson, D. J., 2009. Distinct subsets of unmyelinated primary sensory fibers mediate behavioral responses to noxious thermal and mechanical stimuli. Proc Natl Acad Sci U S A 106, 9075-9080.
- Ceresa, C., Avan, A., Giovannetti, E., Geldof, A. A., Cavaletti, G., Peters, G. J., 2014. Characterization of and protection from neurotoxicity induced by oxaliplatin, bortezomib and epothilone-B. Anticancer Res 34, 517-523.
- Cervetto, L., Demontis, G. C., Gargini, C., 2007. Cellular mechanisms underlying the pharmacological induction of phosphenes. Br J Pharmacol 150, 383-390.
- Chaplan, S. R., Guo, H. Q., Lee, D. H., Luo, L., Liu, C., Kuei, C., Velumian, A. A., Butler, M. P., Brown, S. M., Dubin, A. E., 2003. Neuronal hyperpolarization-activated pacemaker channels drive neuropathic pain. J Neurosci 23, 1169-1178.
- Chen, J., Mitcheson, J. S., Lin, M., Sanguinetti, M. C., 2000. Functional roles of charged residues in the putative voltage sensor of the HCN2 pacemaker channel. J Biol Chem 275, 36465-36471.
- Chen, S., Wang, J., Siegelbaum, S. A., 2001. Properties of hyperpolarization-activated pacemaker current defined by coassembly of HCN1 and HCN2 subunits and basal modulation by cyclic nucleotide. J Gen Physiol 117, 491-504.

- Cheng, Q., Zhou, Y., 2013. Novel role of KT5720 on regulating hyperpolarization-activated cyclic nucleotide-gated channel activity and dorsal root ganglion neuron excitability. DNA Cell Biol 32, 320-328.
- Chevaleyre, V., Castillo, P. E., 2002. Assessing the role of Ih channels in synaptic transmission and mossy fiber LTP. Proc Natl Acad Sci U S A 99, 9538-9543.
- Colbert, C. M., Johnston, D., 1996. Axonal action-potential initiation and Na+ channel densities in the soma and axon initial segment of subicular pyramidal neurons. J Neurosci 16, 6676-6686.
- COOK, A. W., BROWDER, E. J., 1965. FUNCTION OF POSTERIOR COLUMNS IN MAN. Arch Neurol 12, 72-79.
- Cosi, C., Mannaioni, G., Cozzi, A., Carlà, V., Sili, M., Cavone, L., Maratea, D., Moroni, F., 2011. G-protein coupled receptor 35 (GPR35) activation and inflammatory pain: Studies on the antinociceptive effects of kynurenic acid and zaprinast. Neuropharmacology 60, 1227-1231.
- Dalle, C., Eisenach, J. C., 2005. Peripheral block of the hyperpolarization-activated cation current (Ih) reduces mechanical allodynia in animal models of postoperative and neuropathic pain. Reg Anesth Pain Med 30, 243-248.
- Davis, A. M., Inturrisi, C. E., 1999. d-Methadone blocks morphine tolerance and N-methyl-D-aspartate-induced hyperalgesia. J Pharmacol Exp Ther 289, 1048-1053.
- Day, M., Carr, D. B., Ulrich, S., Ilijic, E., Tkatch, T., Surmeier, D. J., 2005. Dendritic excitability of mouse frontal cortex pyramidal neurons is shaped by the interaction among HCN, Kir2, and Kleak channels. J Neurosci 25, 8776-8787.
- de C Williams, A. C., Davies, H. T., Chadury, Y., 2000. Simple pain rating scales hide complex idiosyncratic meanings. Pain 85, 457-463.
- de Castria, T. B., da Silva, E. M., Gois, A. F., Riera, R., 2013. Cisplatin versus carboplatin in combination with third-generation drugs for advanced non-small cell lung cancer. Cochrane Database Syst Rev 8, Cd009256.
- Deng, H., Fang, Y., 2012. Anti-inflammatory gallic Acid and wedelolactone are G protein-coupled receptor-35 agonists. Pharmacology 89, 211-219.
- Descoeur, J., Pereira, V., Pizzoccaro, A., Francois, A., Ling, B., Maffre, V., Couette, B., Busserolles, J., Courteix, C., Noel, J., Lazdunski, M., Eschalier, A., Authier, N., Bourinet, E., 2011. Oxaliplatin-induced cold hypersensitivity is due to remodelling of ion channel expression in nociceptors. EMBO Mol Med 3, 266-278.
- DiFrancesco, D., Ferroni, A., Mazzanti, M., Tromba, C., 1986. Properties of the hyperpolarizing-activated current (if) in cells isolated from the rabbit sino-atrial node. J Physiol 377, 61-88.
- Divorty, N., Mackenzie, A. E., Nicklin, S. A., Milligan, G., 2015. G protein-coupled receptor 35: an emerging target in inflammatory and cardiovascular disease. Front Pharmacol 6, 41.
- Dunlop, J., Vasilyev, D., Lu, P., Cummons, T., Bowlby, M. R., 2009. Hyperpolarization-activated cyclic nucleotide-gated (HCN) channels and pain. Curr Pharm Des 15, 1767-1772.

- Dworkin, R. H., O'Connor, A. B., Audette, J., Baron, R., Gourlay, G. K., Haanpää, M. L., Kent, J. L., Krane, E. J., Lebel, A. A., Levy, R. M., Mackey, S. C., Mayer, J., Miaskowski, C., Raja, S. N., Rice, A. S., Schmader, K. E., Stacey, B., Stanos, S., Treede, R. D., Turk, D. C., Walco, G. A., Wells, C. D., 2010. Recommendations for the pharmacological management of neuropathic pain: an overview and literature update. Mayo Clin Proc 85, S3-14.
- Dyck, P. J., Larson, T. S., O'Brien, P. C., Velosa, J. A., 2000. Patterns of quantitative sensation testing of hypoesthesia and hyperalgesia are predictive of diabetic polyneuropathy: a study of three cohorts. Nerve growth factor study group. Diabetes Care 23, 510-517.
- Dzagnidze, A., Katsarava, Z., Makhalova, J., Liedert, B., Yoon, M. S., Kaube, H., Limmroth, V., Thomale, J., 2007. Repair capacity for platinum-DNA adducts determines the severity of cisplatin-induced peripheral neuropathy. J Neurosci 27, 9451-9457.
- Elias, W. J., Burchiel, K. J., 2002. Microvascular decompression. Clin J Pain 18, 35-41.
- Emery, E. C., Young, G. T., Berrocoso, E. M., Chen, L., McNaughton, P. A., 2011. HCN2 ion channels play a central role in inflammatory and neuropathic pain. Science 333, 1462-1466.
- Emery, E. C., Young, G. T., McNaughton, P. A., 2012. HCN2 ion channels: an emerging role as the pacemakers of pain. Trends Pharmacol Sci 33, 456-463.
- Ezendam, N. P., Pijlman, B., Bhugwandass, C., Pruijt, J. F., Mols, F., Vos, M. C., Pijnenborg, J. M., van de Poll-Franse, L. V., 2014. Chemotherapy-induced peripheral neuropathy and its impact on health-related quality of life among ovarian cancer survivors: results from the population-based PROFILES registry. Gynecol Oncol 135, 510-517.
- Fallarini, S., Magliulo, L., Paoletti, T., de Lalla, C., Lombardi, G., 2010. Expression of functional GPR35 in human iNKT cells. Biochem Biophys Res Commun 398, 420-425.
- Felix, R., Sandoval, A., Sánchez, D., Gómora, J. C., De la Vega-Beltrán, J. L., Treviño, C. L., Darszon, A., 2003. ZD7288 inhibits low-threshold Ca(2+) channel activity and regulates sperm function. Biochem Biophys Res Commun 311, 187-192.
- Finnerup, N. B., Otto, M., Jensen, T. S., Sindrup, S. H., 2007. An evidence-based algorithm for the treatment of neuropathic pain. MedGenMed 9, 36.
- Finnerup, N. B., Otto, M., McQuay, H. J., Jensen, T. S., Sindrup, S. H., 2005. Algorithm for neuropathic pain treatment: an evidence based proposal. Pain 118, 289-305.
- Flatters, S. J., Bennett, G. J., 2006. Studies of peripheral sensory nerves in paclitaxel-induced painful peripheral neuropathy: evidence for mitochondrial dysfunction. Pain 122, 245-257.
- Franz, O., Liss, B., Neu, A., Roeper, J., 2000. Single-cell mRNA expression of HCN1 correlates with a fast gating phenotype of hyperpolarization-activated cyclic nucleotide-gated ion channels (Ih) in central neurons. Eur J Neurosci 12, 2685-2693.

- Fuertes, M. A., Castilla, J., Alonso, C., Perez, J. M., 2002. Novel concepts in the development of platinum antitumor drugs. Curr Med Chem Anticancer Agents 2, 539-551.
- Gao, L. L., McMullan, S., Djouhri, L., Acosta, C., Harper, A. A., Lawson, S. N., 2012. Expression and properties of hyperpolarization-activated current in rat dorsal root ganglion neurons with known sensory function. J Physiol 590, 4691-4705.
- Gasparini, S., DiFrancesco, D., 1997. Action of the hyperpolarization-activated current (Ih) blocker ZD 7288 in hippocampal CA1 neurons. Pflugers Arch 435, 99-106.
- Ghelardini, C., Desaphy, J. F., Muraglia, M., Corbo, F., Matucci, R., Dipalma, A., Bertucci, C., Pistolozzi, M., Nesi, M., Norcini, M., Franchini, C., Camerino, D. C., 2010. Effects of a new potent analog of tocainide on hNav1.7 sodium channels and in vivo neuropathic pain models. Neuroscience 169, 863-873.
- Gregg, R. W., Molepo, J. M., Monpetit, V. J., Mikael, N. Z., Redmond, D., Gadia, M., Stewart, D. J., 1992. Cisplatin neurotoxicity: the relationship between dosage, time, and platinum concentration in neurologic tissues, and morphologic evidence of toxicity. J Clin Oncol 10, 795-803.
- Grothey, A., Goldberg, R. M., 2004. A review of oxaliplatin and its clinical use in colorectal cancer. Expert Opin Pharmacother 5, 2159-2170.
- Guo, J., Williams, D. J., Puhl, H. L., Ikeda, S. R., 2008. Inhibition of N-type calcium channels by activation of GPR35, an orphan receptor, heterologously expressed in rat sympathetic neurons. J Pharmacol Exp Ther 324, 342-351.
- Gureje, O., 2007. Psychiatric aspects of pain. Curr Opin Psychiatry 20, 42-46.
- Hammond, C., Ammari, R., Bioulac, B., Garcia, L., 2008. Latest view on the mechanism of action of deep brain stimulation. Mov Disord 23, 2111-2121.
- Hansen, N., Uçeyler, N., Palm, F., Zelenka, M., Biko, L., Lesch, K. P., Gerlach, M., Sommer, C., 2011. Serotonin transporter deficiency protects mice from mechanical allodynia and heat hyperalgesia in vincristine neuropathy. Neurosci Lett 495, 93-97.
- Hearn, L., Moore, R. A., Derry, S., Wiffen, P. J., Phillips, T., 2014. Desipramine for neuropathic pain in adults. Cochrane Database Syst Rev 9, CD011003.
- Herrmann, S., Schnorr, S., Ludwig, A., 2015. HCN channels--modulators of cardiac and neuronal excitability. Int J Mol Sci 16, 1429-1447.
- Hershman, D. L., Lacchetti, C., Dworkin, R. H., Lavoie Smith, E. M., Bleeker, J., Cavaletti, G., Chauhan, C., Gavin, P., Lavino, A., Lustberg, M. B., Paice, J., Schneider, B., Smith, M. L., Smith, T., Terstriep, S., Wagner-Johnston, N., Bak, K., Loprinzi, C. L., 2014. Prevention and management of chemotherapy-induced peripheral neuropathy in survivors of adult cancers: American Society of Clinical Oncology clinical practice guideline. J Clin Oncol 32, 1941-1967.
- Holland, N. R., Stocks, A., Hauer, P., Cornblath, D. R., Griffin, J. W., McArthur, J. C., 1997. Intraepidermal nerve fiber density in patients with painful sensory neuropathy. Neurology 48, 708-711.

- Huang, Z., Lujan, R., Kadurin, I., Uebele, V. N., Renger, J. J., Dolphin, A. C., Shah, M. M., 2011. Presynaptic HCN1 channels regulate Cav3.2 activity and neurotransmission at select cortical synapses. Nat Neurosci 14, 478-486.
- Häusser, M., Clark, B. A., 1997. Tonic synaptic inhibition modulates neuronal output pattern and spatiotemporal synaptic integration. Neuron 19, 665-678.
- Ibrahim, A., Hirschfeld, S., Cohen, M. H., Griebel, D. J., Williams, G. A., Pazdur, R., 2004. FDA drug approval summaries: oxaliplatin. Oncologist 9, 8-12.
- Jaffe, D. B., Carnevale, N. T., 1999. Passive normalization of synaptic integration influenced by dendritic architecture. J Neurophysiol 82, 3268-3285.
- Jafri, M. S., Weinreich, D., 1998. Substance P regulates Ih via a NK-1 receptor in vagal sensory neurons of the ferret. J Neurophysiol 79, 769-777.
- Jamieson, S. M., Liu, J. J., Connor, B., Dragunow, M., McKeage, M. J., 2007. Nucleolar enlargement, nuclear eccentricity and altered cell body immunostaining characteristics of large-sized sensory neurons following treatment of rats with paclitaxel. Neurotoxicology 28, 1092-1098.
- Jenkins, L., Harries, N., Lappin, J. E., MacKenzie, A. E., Neetoo-Isseljee, Z., Southern, C., McIver, E. G., Nicklin, S. A., Taylor, D. L., Milligan, G., 2012. Antagonists of GPR35 display high species ortholog selectivity and varying modes of action. J Pharmacol Exp Ther 343, 683-695.
- Jiang, Y. Q., Sun, Q., Tu, H. Y., Wan, Y., 2008a. Characteristics of HCN channels and their participation in neuropathic pain. Neurochem Res 33, 1979-1989.
- Jiang, Y. Q., Xing, G. G., Wang, S. L., Tu, H. Y., Chi, Y. N., Li, J., Liu, F. Y., Han, J. S., Wan, Y., 2008b. Axonal accumulation of hyperpolarization-activated cyclic nucleotide-gated cation channels contributes to mechanical allodynia after peripheral nerve injury in rat. Pain 137, 495-506.
- Kandel, E. R., Schwartz, J. H., Jessel, T. M., 2013. Principles of neural science, fifth edition. McGraw-Hill Medical, New York.
- Kennedy, J. D., 2007. Neuropathic pain: molecular complexity underlies continuing unmet medical need. J Med Chem 50, 2547-2556.
- Kim, J. H., Dougherty, P. M., Abdi, S., 2015. Basic science and clinical management of painful and non-painful chemotherapy-related neuropathy. Gynecol Oncol 136, 453-459.
- Krishnan, A. V., Goldstein, D., Friedlander, M., Kiernan, M. C., 2006. Oxaliplatin and axonal Na+ channel function in vivo. Clin Cancer Res 12, 4481-4484.
- Lees-Miller, J. P., Guo, J., Wang, Y., Perissinotti, L. L., Noskov, S. Y., Duff, H. J., 2015. Ivabradine prolongs phase 3 of cardiac repolarization and blocks the hERG1 (KCNH2) current over a concentration-range overlapping with that required to block HCN4. J Mol Cell Cardiol 85, 71-78.
- Leighton, G. E., Rodriguez, R. E., Hill, R. G., Hughes, J., 1988. kappa-Opioid agonists produce antinociception after i.v. and i.c.v. but not intrathecal administration in the rat. Br J Pharmacol 93, 553-560.
- Li, Y., Dorsi, M. J., Meyer, R. A., Belzberg, A. J., 2000. Mechanical hyperalgesia after an L5 spinal nerve lesion in the rat is not dependent on input from injured nerve fibers. Pain 85, 493-502.

- Liu, J. J., Kim, Y., Yan, F., Ding, Q., Ip, V., Jong, N. N., Mercer, J. F., McKeage, M. J., 2013. Contributions of rat Ctr1 to the uptake and toxicity of copper and platinum anticancer drugs in dorsal root ganglion neurons. Biochem Pharmacol 85, 207-215.
- Ludwig, A., Zong, X., Jeglitsch, M., Hofmann, F., Biel, M., 1998. A family of hyperpolarization-activated mammalian cation channels. Nature 393, 587-591.
- Lynch, S. S., Cheng, C. M., Yee, J. L., 2006. Intrathecal ziconotide for refractory chronic pain. Ann Pharmacother 40, 1293-1300.
- Lörincz, A., Notomi, T., Tamás, G., Shigemoto, R., Nusser, Z., 2002. Polarized and compartment-dependent distribution of HCN1 in pyramidal cell dendrites. Nat Neurosci 5, 1185-1193.
- Maccaferri, G., McBain, C. J., 1996. The hyperpolarization-activated current (Ih) and its contribution to pacemaker activity in rat CA1 hippocampal stratum oriens-alveus interneurones. J Physiol 497 (Pt 1), 119-130.
- MacKenzie, A. E., Caltabiano, G., Kent, T. C., Jenkins, L., McCallum, J. E., Hudson, B. D., Nicklin, S. A., Fawcett, L., Markwick, R., Charlton, S. J., Milligan, G., 2014. The antiallergic mast cell stabilizers lodoxamide and bufrolin as the first high and equipotent agonists of human and rat GPR35. Mol Pharmacol 85, 91-104.
- Mackenzie, A. E., Milligan, G., 2015. The emerging pharmacology and function of GPR35 in the nervous system. Neuropharmacology.
- Macri, V., Accili, E. A., 2004. Structural elements of instantaneous and slow gating in hyperpolarization-activated cyclic nucleotide-gated channels. J Biol Chem 279, 16832-16846.
- Macri, V., Proenza, C., Agranovich, E., Angoli, D., Accili, E. A., 2002. Separable gating mechanisms in a Mammalian pacemaker channel. J Biol Chem 277, 35939-35946.
- Magee, J. C., 1998. Dendritic hyperpolarization-activated currents modify the integrative properties of hippocampal CA1 pyramidal neurons. J Neurosci 18, 7613-7624.
- Magee, J. C., 1999. Dendritic Ih normalizes temporal summation in hippocampal CA1 neurons. Nat Neurosci 2, 848.
- Magee, J. C., 2000. Dendritic integration of excitatory synaptic input. Nat Rev Neurosci 1, 181-190.
- Main, C. J., Spanswick, C. C., 2000. Pain management : an interdisciplinary approach. Churchill Livingstone, Edinburgh ; New York.
- Mainen, Z. F., Sejnowski, T. J., 1996. Influence of dendritic structure on firing pattern in model neocortical neurons. Nature 382, 363-366.
- Maravillas-Montero, J. L., Burkhardt, A. M., Hevezi, P. A., Carnevale, C. D., Smit, M. J., Zlotnik, A., 2015. Cutting edge: GPR35/CXCR8 is the receptor of the mucosal chemokine CXCL17. J Immunol 194, 29-33.
- Martindale, J., Bland-Ward, P. A., Chessell, I. P., 2001. Inhibition of C-fibre mediated sensory transmission in the rat following intraplantar formalin. Neurosci Lett 316, 33-36.
- Massey, R. L., Kim, H. K., Abdi, S., 2014. Brief review: chemotherapy-induced painful peripheral neuropathy (CIPPN): current status and future directions. Can J Anaesth 61, 754-762.

- Matsumoto, G., Ichikawa, M., Tasaki, A., Murofushi, H., Sakai, H., 1984. Axonal microtubules necessary for generation of sodium current in squid giant axons: I. Pharmacological study on sodium current and restoration of sodium current by microtubule proteins and 260K protein. J Membr Biol 77, 77-91.
- Mayer, D. J., Wolfle, T. L., Akil, H., Carder, B., Liebeskind, J. C., 1971. Analgesia from electrical stimulation in the brainstem of the rat. Science 174, 1351-1354.
- Mayer, M. L., Westbrook, G. L., 1983. A voltage-clamp analysis of inward (anomalous) rectification in mouse spinal sensory ganglion neurones. J Physiol 340, 19-45.
- McCall, W. D., Tanner, K. D., Levine, J. D., 1996. Formalin induces biphasic activity in C-fibers in the rat. Neurosci Lett 208, 45-48.
- McDonald, E. S., Randon, K. R., Knight, A., Windebank, A. J., 2005. Cisplatin preferentially binds to DNA in dorsal root ganglion neurons in vitro and in vivo: a potential mechanism for neurotoxicity. Neurobiol Dis 18, 305-313.
- Meijer, C., de Vries, E. G., Marmiroli, P., Tredici, G., Frattola, L., Cavaletti, G., 1999. Cisplatin-induced DNA-platination in experimental dorsal root ganglia neuronopathy. Neurotoxicology 20, 883-887.
- Merskey, H., Bogduk, N., 1994. Part III: Pain Terms, A Current List with Definitions and Notes on Usage. Classification of Chronic Pain, Second Edition, International Association for the study of Pain (IASP) Task Force on Taxonomy, Seattle, pp. pp 209-214.
- Michel, M. C., Wieland, T., Tsujimoto, G., 2009. How reliable are G-protein-coupled receptor antibodies? Naunyn Schmiedebergs Arch Pharmacol 379, 385-388.
- Milligan, G., 2011. Orthologue selectivity and ligand bias: translating the pharmacology of GPR35. Trends Pharmacol Sci 32, 317-325.
- Min, K. D., Asakura, M., Liao, Y., Nakamaru, K., Okazaki, H., Takahashi, T., Fujimoto, K., Ito, S., Takahashi, A., Asanuma, H., Yamazaki, S., Minamino, T., Sanada, S., Seguchi, O., Nakano, A., Ando, Y., Otsuka, T., Furukawa, H., Isomura, T., Takashima, S., Mochizuki, N., Kitakaze, M., 2010. Identification of genes related to heart failure using global gene expression profiling of human failing myocardium. Biochem Biophys Res Commun 393, 55-60.
- Mixcoatl-Zecuatl, T., Aguirre-Bañuelos, P., Granados-Soto, V., 2000. Sildenafil produces antinociception and increases morphine antinociception in the formalin test. Eur J Pharmacol 400, 81-87.
- Mollman, J. E., 1990. Cisplatin neurotoxicity. N Engl J Med 322, 126-127.
- Momin, A., Cadiou, H., Mason, A., McNaughton, P. A., 2008. Role of the hyperpolarization-activated current Ih in somatosensory neurons. J Physiol 586, 5911-5929.
- Moore, R. A., Derry, S., Aldington, D., Cole, P., Wiffen, P. J., 2012. Amitriptyline for neuropathic pain and fibromyalgia in adults. Cochrane Database Syst Rev 12, CD008242.
- Moosmang, S., Biel, M., Hofmann, F., Ludwig, A., 1999. Differential distribution of four hyperpolarization-activated cation channels in mouse brain. Biol Chem 380, 975-980.

- Muthuraman, A., Jaggi, A. S., Singh, N., Singh, D., 2008. Ameliorative effects of amiloride and pralidoxime in chronic constriction injury and vincristine induced painful neuropathy in rats. Eur J Pharmacol 587, 104-111.
- Nelson, K. A., Park, K. M., Robinovitz, E., Tsigos, C., Max, M. B., 1997. High-dose oral dextromethorphan versus placebo in painful diabetic neuropathy and postherpetic neuralgia. Neurology 48, 1212-1218.
- Nolan, M. F., Malleret, G., Lee, K. H., Gibbs, E., Dudman, J. T., Santoro, B., Yin, D., Thompson, R. F., Siegelbaum, S. A., Kandel, E. R., Morozov, A., 2003. The hyperpolarization-activated HCN1 channel is important for motor learning and neuronal integration by cerebellar Purkinje cells. Cell 115, 551-564.
- Nolano, M., Simone, D. A., Wendelschafer-Crabb, G., Johnson, T., Hazen, E., Kennedy, W. R., 1999. Topical capsaicin in humans: parallel loss of epidermal nerve fibers and pain sensation. Pain 81, 135-145.
- Noma, A., Irisawa, H., 1976. A time- and voltage-dependent potassium current in the rabbit sinoatrial node cell. Pflugers Arch 366, 251-258.
- Notomi, T., Shigemoto, R., 2004. Immunohistochemical localization of Ih channel subunits, HCN1-4, in the rat brain. J Comp Neurol 471, 241-276.
- O'Dowd, B. F., Nguyen, T., Marchese, A., Cheng, R., Lynch, K. R., Heng, H. H., Kolakowski, L. F., George, S. R., 1998. Discovery of three novel G-protein-coupled receptor genes. Genomics 47, 310-313.
- Ohshiro, H., Tonai-Kachi, H., Ichikawa, K., 2008. GPR35 is a functional receptor in rat dorsal root ganglion neurons. Biochem Biophys Res Commun 365, 344-348.
- Oka, S., Ota, R., Shima, M., Yamashita, A., Sugiura, T., 2010. GPR35 is a novel lysophosphatidic acid receptor. Biochem Biophys Res Commun 395, 232-237.
- Okumura, S., Baba, H., Kumada, T., Nanmoku, K., Nakajima, H., Nakane, Y., Hioki, K., Ikenaka, K., 2004. Cloning of a G-protein-coupled receptor that shows an activity to transform NIH3T3 cells and is expressed in gastric cancer cells. Cancer Sci 95, 131-135.
- Olivi, A., Gilbert, M., Duncan, K. L., Corden, B., Lenartz, D., Brem, H., 1993. Direct delivery of platinum-based antineoplastics to the central nervous system: a toxicity and ultrastructural study. Cancer Chemother Pharmacol 31, 449-454.
- Pape, H. C., 1996. Queer current and pacemaker: the hyperpolarization-activated cation current in neurons. Annu Rev Physiol 58, 299-327.
- Papp, I., Hollo, K., Antal, M., 2010. Plasticity of hyperpolarization-activated and cyclic nucleotid-gated cation channel subunit 2 expression in the spinal dorsal horn in inflammatory pain. Eur J Neurosci 32, 1193-1201.
- Papp, I., Szucs, P., Hollo, K., Erdelyi, F., Szabo, G., Antal, M., 2006. Hyperpolarization-activated and cyclic nucleotide-gated cation channel subunit 2 ion channels modulate synaptic transmission from nociceptive primary afferents containing substance P to secondary sensory neurons in laminae I-IIo of the rodent spinal dorsal horn. Eur J Neurosci 24, 1341-1352.
- Park, S. B., Krishnan, A. V., Lin, C. S., Goldstein, D., Friedlander, M., Kiernan, M. C., 2008. Mechanisms underlying chemotherapy-induced

neurotoxicity and the potential for neuroprotective strategies. Curr Med Chem 15, 3081-3094.
- Park, S. B., Lin, C. S., Krishnan, A. V., Goldstein, D., Friedlander, M. L., Kiernan, M. C., 2009. Oxaliplatin-induced neurotoxicity: changes in axonal excitability precede development of neuropathy. Brain 132, 2712-2723.
- Perkins, K. L., Wong, R. K., 1995. Intracellular QX-314 blocks the hyperpolarization-activated inward current Iq in hippocampal CA1 pyramidal cells. J Neurophysiol 73, 911-915.
- Pettit, D. L., Augustine, G. J., 2000. Distribution of functional glutamate and GABA receptors on hippocampal pyramidal cells and interneurons. J Neurophysiol 84, 28-38.
- Pian, P., Bucchi, A., Decostanzo, A., Robinson, R. B., Siegelbaum, S. A., 2007. Modulation of cyclic nucleotide-regulated HCN channels by PIP(2) and receptors coupled to phospholipase C. Pflugers Arch 455, 125-145.
- Podratz, J. L., Knight, A. M., Ta, L. E., Staff, N. P., Gass, J. M., Genelin, K., Schlattau, A., Lathroum, L., Windebank, A. J., 2011. Cisplatin induced mitochondrial DNA damage in dorsal root ganglion neurons. Neurobiol Dis 41, 661-668.
- Poolos, N. P., Bullis, J. B., Roth, M. K., 2006. Modulation of h-channels in hippocampal pyramidal neurons by p38 mitogen-activated protein kinase. J Neurosci 26, 7995-8003.
- Rahaman, J., Steiner, N., Hayes, M. P., Chuang, L., Fishman, D., Gretz Iii, H., 2009. Chemotherapy for gynecologic cancers. Mt Sinai J Med 76, 577-588.
- Robinson, R. B., Siegelbaum, S. A., 2003. Hyperpolarization-activated cation currents: from molecules to physiological function. Annu Rev Physiol 65, 453-480.
- Ronkainen, V. P., Tuomainen, T., Huusko, J., Laidinen, S., Malinen, M., Palvimo, J. J., Ylä-Herttuala, S., Vuolteenaho, O., Tavi, P., 2014. Hypoxia-inducible factor 1-induced G protein-coupled receptor 35 expression is an early marker of progressive cardiac remodelling. Cardiovasc Res 101, 69-77.
- Sakurai, M., Egashira, N., Kawashiri, T., Yano, T., Ikesue, H., Oishi, R., 2009. Oxaliplatin-induced neuropathy in the rat: involvement of oxalate in cold hyperalgesia but not mechanical allodynia. Pain 147, 165-174.
- Santoro, B., Chen, S., Luthi, A., Pavlidis, P., Shumyatsky, G. P., Tibbs, G. R., Siegelbaum, S. A., 2000. Molecular and functional heterogeneity of hyperpolarization-activated pacemaker channels in the mouse CNS. J Neurosci 20, 5264-5275.
- Santoro, B., Liu, D. T., Yao, H., Bartsch, D., Kandel, E. R., Siegelbaum, S. A., Tibbs, G. R., 1998. Identification of a gene encoding a hyperpolarization-activated pacemaker channel of brain. Cell 93, 717-729.
- Schnorr, S., Eberhardt, M., Kistner, K., Rajab, H., Käßer, J., Hess, A., Reeh, P., Ludwig, A., Herrmann, S., 2014. HCN2 channels account for mechanical (but not heat) hyperalgesia during long-standing inflammation. Pain 155, 1079-1090.
- Scroggs, R. S., Todorovic, S. M., Anderson, E. G., Fox, A. P., 1994. Variation in IH, IIR, and ILEAK between acutely isolated adult rat dorsal root ganglion neurons of different size. J Neurophysiol 71, 271-279.

- Semenchuk, M. R., Davis, B., 2000. Efficacy of sustained-release bupropion in neuropathic pain: an open-label study. Clin J Pain 16, 6-11.
- Semenchuk, M. R., Sherman, S., Davis, B., 2001. Double-blind, randomized trial of bupropion SR for the treatment of neuropathic pain. Neurology 57, 1583-1588.
- Shah, T. H., Moradimehr, A., 2010. Bupropion for the treatment of neuropathic pain. Am J Hosp Palliat Care 27, 333-336.
- Shin, M., Chetkovich, D. M., 2007. Activity-dependent regulation of h channel distribution in hippocampal CA1 pyramidal neurons. J Biol Chem 282, 33168-33180.
- Shore, D. M., Reggio, P. H., 2015. The therapeutic potential of orphan GPCRs, GPR35 and GPR55. Front Pharmacol 6, 69.
- Siau, C., Xiao, W., Bennett, G. J., 2006. Paclitaxel- and vincristine-evoked painful peripheral neuropathies: loss of epidermal innervation and activation of Langerhans cells. Exp Neurol 201, 507-514.
- Smith, E. M., Pang, H., Cirrincione, C., Fleishman, S., Paskett, E. D., Ahles, T., Bressler, L. R., Fadul, C. E., Knox, C., Le-Lindqwister, N., Gilman, P. B., Shapiro, C. L., Oncology, A. f. C. T. i., 2013. Effect of duloxetine on pain, function, and quality of life among patients with chemotherapy-induced painful peripheral neuropathy: a randomized clinical trial. JAMA 309, 1359-1367.
- Southern, C., Cook, J. M., Neetoo-Isseljee, Z., Taylor, D. L., Kettleborough, C. A., Merritt, A., Bassoni, D. L., Raab, W. J., Quinn, E., Wehrman, T. S., Davenport, A. P., Brown, A. J., Green, A., Wigglesworth, M. J., Rees, S., 2013. Screening β-arrestin recruitment for the identification of natural ligands for orphan G-protein-coupled receptors. J Biomol Screen 18, 599-609.
- Sprowl, J. A., Ciarimboli, G., Lancaster, C. S., Giovinazzo, H., Gibson, A. A., Du, G., Janke, L. J., Cavaletti, G., Shields, A. F., Sparreboom, A., 2013. Oxaliplatin-induced neurotoxicity is dependent on the organic cation transporter OCT2. Proc Natl Acad Sci U S A 110, 11199-11204.
- Sun, X., Windebank, A. J., 1996. Calcium in suramin-induced rat sensory neuron toxicity in vitro. Brain Res 742, 149-156.
- Sánchez-Alonso, J. L., Halliwell, J. V., Colino, A., 2008. ZD 7288 inhibits T-type calcium current in rat hippocampal pyramidal cells. Neurosci Lett 439, 275-280.
- Takasu, K., Ono, H., Tanabe, M., 2010. Spinal hyperpolarization-activated cyclic nucleotide-gated cation channels at primary afferent terminals contribute to chronic pain. Pain 151, 87-96.
- Taniguchi, Y., Tonai-Kachi, H., Shinjo, K., 2006. Zaprinast, a well-known cyclic guanosine monophosphate-specific phosphodiesterase inhibitor, is an agonist for GPR35. FEBS Lett 580, 5003-5008.
- Tao, F., Tao, Y. X., Zhao, C., Doré, S., Liaw, W. J., Raja, S. N., Johns, R. A., 2004. Differential roles of neuronal and endothelial nitric oxide synthases during carrageenan-induced inflammatory hyperalgesia. Neuroscience 128, 421-430.
- Thimm, D., Funke, M., Meyer, A., Müller, C. E., 2013. 6-Bromo-8-(4-[(3)H]methoxybenzamido)-4-oxo-4H-chromene-2-carboxylic Acid: a

powerful tool for studying orphan G protein-coupled receptor GPR35. J Med Chem 56, 7084-7099.
- Torrance, N., Smith, B. H., Bennett, M. I., Lee, A. J., 2006. The epidemiology of chronic pain of predominantly neuropathic origin. Results from a general population survey. J Pain 7, 281-289.
- Turk, D., Okifuji, A., 2001. Pain Terms and Taxonomies of Pain. Lippincott Williams & Wilkins, pp. 17-25.
- Turner, J. A., Loeser, J. D., Deyo, R. A., Sanders, S. B., 2004. Spinal cord stimulation for patients with failed back surgery syndrome or complex regional pain syndrome: a systematic review of effectiveness and complications. Pain 108, 137-147.
- Turner, J. A., Sears, J. M., Loeser, J. D., 2007. Programmable intrathecal opioid delivery systems for chronic noncancer pain: a systematic review of effectiveness and complications. Clin J Pain 23, 180-195.
- Vaccarino, A. L., Marek, P., Kest, B., Weber, E., Keana, J. F., Liebeskind, J. C., 1993. NMDA receptor antagonists, MK-801 and ACEA-1011, prevent the development of tonic pain following subcutaneous formalin. Brain Res 615, 331-334.
- Vellani, V., Zachrisson, O., McNaughton, P. A., 2004. Functional bradykinin B1 receptors are expressed in nociceptive neurones and are upregulated by the neurotrophin GDNF. J Physiol 560, 391-401.
- Verstappen, C. C., Heimans, J. J., Hoekman, K., Postma, T. J., 2003. Neurotoxic complications of chemotherapy in patients with cancer: clinical signs and optimal management. Drugs 63, 1549-1563.
- Wall, P. D., McMahon, S. B., Koltzenburg, M., 2006. Wall and Melzack's textbook of pain. Elsevier/Churchill Livingstone, Philadelphia.
- Wang, J., Simonavicius, N., Wu, X., Swaminath, G., Reagan, J., Tian, H., Ling, L., 2006. Kynurenic acid as a ligand for orphan G protein-coupled receptor GPR35. J Biol Chem 281, 22021-22028.
- Watts, A. E., Williams, J. T., Henderson, G., 1996. Baclofen inhibition of the hyperpolarization-activated cation current, Ih, in rat substantia nigra zona compacta neurons may be secondary to potassium current activation. J Neurophysiol 76, 2262-2270.
- Weiner, R. S., 2002. Pain management : a practical guide for clinicians. CRC Press, Boca Raton.
- Wells, J. E., Rowland, K. C., Proctor, E. K., 2007. Hyperpolarization-activated channels in trigeminal ganglia innervating healthy and pulp-exposed teeth. Int Endod J 40, 715-721.
- Weng, X., Smith, T., Sathish, J., Djouhri, L., 2012. Chronic inflammatory pain is associated with increased excitability and hyperpolarization-activated current (Ih) in C- but not Adelta-nociceptors. Pain 153, 900-914.
- Wheeler, D. B., Randall, A., Tsien, R. W., 1994. Roles of N-type and Q-type Ca2+ channels in supporting hippocampal synaptic transmission. Science 264, 107-111.
- Wiffen, P. J., Derry, S., Moore, R. A., 2013. Lamotrigine for chronic neuropathic pain and fibromyalgia in adults. Cochrane Database Syst Rev 12, CD006044.

- Wilson, R. H., Lehky, T., Thomas, R. R., Quinn, M. G., Floeter, M. K., Grem, J. L., 2002. Acute oxaliplatin-induced peripheral nerve hyperexcitability. J Clin Oncol 20, 1767-1774.
- Wollmuth, L. P., Hille, B., 1992. Ionic selectivity of Ih channels of rod photoreceptors in tiger salamanders. J Gen Physiol 100, 749-765.
- Womble, M. D., Moises, H. C., 1993. Hyperpolarization-activated currents in neurons of the rat basolateral amygdala. J Neurophysiol 70, 2056-2065.
- Woolf, C. J., 2010. What is this thing called pain? J Clin Invest 120, 3742-3744.
- Xu, X., Weksler-Zangen, S., Pikarsky, A., Pappo, O., Wengrower, D., Bischoff, S. C., Pines, M., Rivkind, A., Goldin, E., Levi-Schaffer, F., 2002. Mast cells involvement in the inflammation and fibrosis development of the TNBS-induced rat model of colitis. Scand J Gastroenterol 37, 330-337.
- Yamasaki, M., Makino, T., Masuzawa, T., Kurokawa, Y., Miyata, H., Takiguchi, S., Nakajima, K., Fujiwara, Y., Matsuura, N., Mori, M., Doki, Y., 2011. Role of multidrug resistance protein 2 (MRP2) in chemoresistance and clinical outcome in oesophageal squamous cell carcinoma. Br J Cancer 104, 707-713.
- Yanagihara, K., Irisawa, H., 1980. Inward current activated during hyperpolarization in the rabbit sinoatrial node cell. Pflugers Arch 385, 11-19.
- Yang, Y., Lu, J. Y., Wu, X., Summer, S., Whoriskey, J., Saris, C., Reagan, J. D., 2010. G-protein-coupled receptor 35 is a target of the asthma drugs cromolyn disodium and nedocromil sodium. Pharmacology 86, 1-5.
- Yao, H., Donnelly, D. F., Ma, C., LaMotte, R. H., 2003. Upregulation of the hyperpolarization-activated cation current after chronic compression of the dorsal root ganglion. J Neurosci 23, 2069-2074.
- Yoon, M. H., Choi, J. I., Bae, H. B., Jeong, S. W., Chung, S. S., Yoo, K. Y., Jeong, C. Y., Kim, S. J., Chung, S. T., Kim, C. M., 2005. Lack of the nitric oxide-cyclic GMP-potassium channel pathway for the antinociceptive effect of intrathecal zaprinast in a rat formalin test. Neurosci Lett 390, 114-117.
- Young, G. T., Emery, E. C., Mooney, E. R., Tsantoulas, C., McNaughton, P. A., 2014. Inflammatory and neuropathic pain are rapidly suppressed by peripheral block of hyperpolarisation-activated cyclic nucleotide-gated ion channels. Pain 155, 1708-1719.
- Yu, F. H., Catterall, W. A., 2004. The VGL-chanome: a protein superfamily specialized for electrical signaling and ionic homeostasis. Sci STKE 2004, re15.
- Zhang, H., Boyette-Davis, J. A., Kosturakis, A. K., Li, Y., Yoon, S. Y., Walters, E. T., Dougherty, P. M., 2013. Induction of monocyte chemoattractant protein-1 (MCP-1) and its receptor CCR2 in primary sensory neurons contributes to paclitaxel-induced peripheral neuropathy. J Pain 14, 1031-1044.
- Zhang, H., Dougherty, P. M., 2014. Enhanced excitability of primary sensory neurons and altered gene expression of neuronal ion channels in dorsal root ganglion in paclitaxel-induced peripheral neuropathy. Anesthesiology 120, 1463-1475.
- Zhao, P., Abood, M. E., 2013. GPR55 and GPR35 and their relationship to cannabinoid and lysophospholipid receptors. Life Sci 92, 453-457.

- Zolles, G., Klöcker, N., Wenzel, D., Weisser-Thomas, J., Fleischmann, B. K., Roeper, J., Fakler, B., 2006. Pacemaking by HCN channels requires interaction with phosphoinositides. Neuron 52, 1027-1036.